EVALUATION OF FILTERS FOR SERIAL GENERATION OF MSK SIGNAL

by

PATRICK R. TATUM

B. S., Kansas State University, 1979

A MASTER'S THESIS

submitted in partial fulfillment of the

requirements for the degree

MASTER OF SCIENCE

Department of Electrical Engineering

KANSAS STATE UNIVERSITY
Manhattan, Kansas

1981

Approved by:

Donald R. Hummels
Major Professor

TABLE OF CONTENTS

LIST OF FIGURES

LIST OF FIGURES
(continued)

EVALUATION OF FILTERS FOR SERIAL GENERATION OF MSK SIGNAL

I. INTRODUCTION

Minimum shift keying (MSK), a relatively new modulation scheme, offers efficient use of power spectrum as well as constant envelope and phase coherence between transmissions. MSK was first generated using a scheme very much like an offset quadri-phase shift keyed (OQPSK) modulator. With the parallel approach, the data is first split into two offset bit streams and then specially shaped prior to modulating the in-phase and quadrature channels.

A more recent approach to MSK, called Serial MSK (SMSK), generates the signal by inputing the data serially into a biphase shift-keyed (BPSK) modulator. The modulator output is then shaped appropriately by a filter which will be referred to in this paper as the ideal SMSK filter.

The ideal SMSK filter has an impulse response which is fairly complicated to synthesize exactly although good approximations have been built. This paper discusses two possible alternative filters which are simple and inexpensive to construct.

A more detailed discussion of MSK and SMSK generation is given in sections II and III respectively and an equivalent low-pass representation of an SMSK communication system is developed in section IV. The representation is convenient for computer applications and many properties of the SMSK system are evaluated using this model. The two filters, a Butterworth filter and a cascaded filter consisting of a Butterworth followed by a double-notch filter, are developed in section V. Included is an evaluation of performance as compared to ideal MSK. The results were enlightening as both configurations offered nearly the same high communications efficiency as ideal MSK.

II. SERIAL MSK

Minimum Shift Keying

MSK was developed by Doelz and Heald [1] back in 1961. It can be viewed as continuous phase frequency shift keying (CPFSK) with a low deviation ratio (mark and space frequencies differ by exactly 1/2 the bit rate) or as an offset quadri-phase shift keyed signal with sinusoidal pulse weighting.

Phase continuity at the bit transitions in the transmitted signal (Figure 1) and a constant envelope are properties characteristic of MSK.

The phase coherent FSK signal consists of two frequencies, f_1 and f_2, denoted the "mark" and "space" frequencies respectively. The two frequencies have a deviation ratio of only 1/2T, hence the name "minimum" shift keying. For some integer n, f_1 and f_2 are given by

$$f_2 = \frac{n+1}{2T} \; ; \quad f_1 = \frac{n}{2T} \quad .$$

For random data transmission, the resulting power spectrum will be centered on the apparent carrier, $f_c = (2n+1)/4T$. Figure 2 shows the compact power spectrum of MSK as compared to another common modulation scheme, OQPSK.

A typical MSK system is shown in Figure 3. The bit streams, $a_I(t)$ and $a_Q(t)$, are generated in parallel, offset by T seconds, and each symbol lasts 2T seconds. The bit streams are multipled by two pulse shaping functions, x(t) and y(t), forming the in-phase and quadrature channels referred to earlier. The shaping functions are offset by 90° so they may be added, transmitted and separated again without distortion.

At the demodulator, the received signal is multiplied by in-phase and quadrature reference signals to separate the signal. It is then sent to the integrate and dump (I and D) circuit. This circuit supplies a low frequency signal to the sychronized sampler. The polarity of the samplers then determine the values of their respective bit streams. Note that the

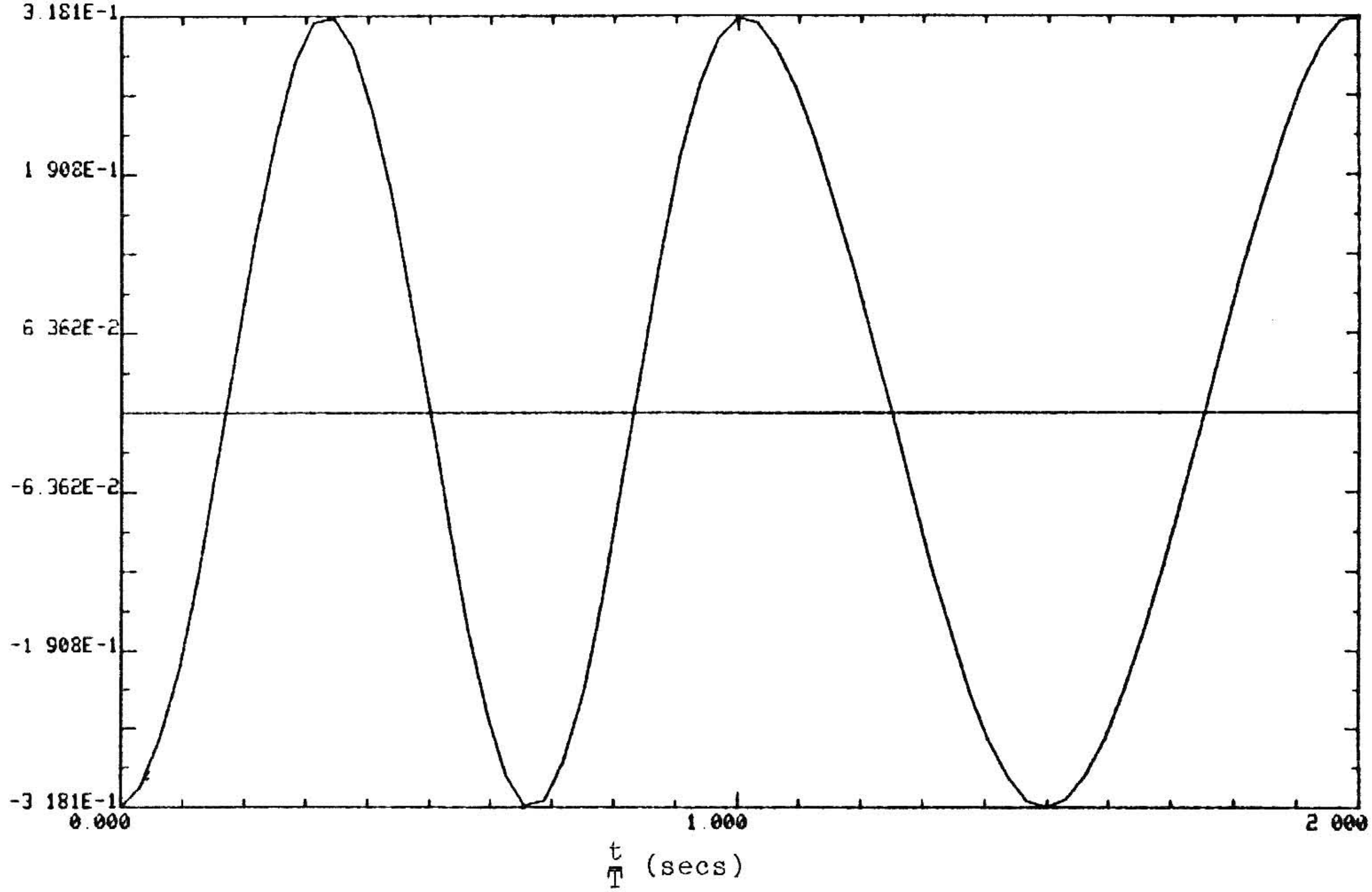

Figure 1. Transmitted MSK Signal

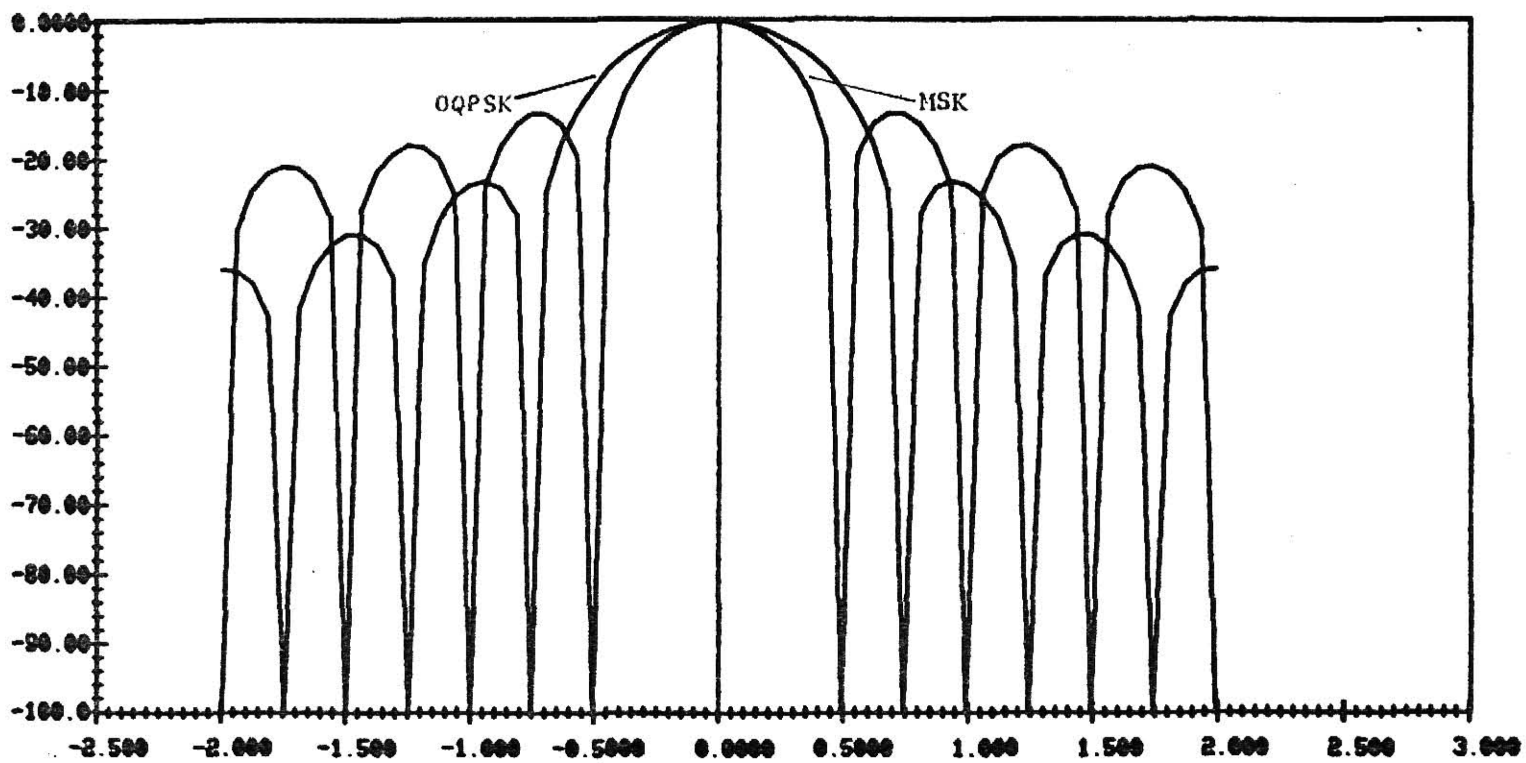

Figure 2. MSK and OQPSK Normalized Power Spectra

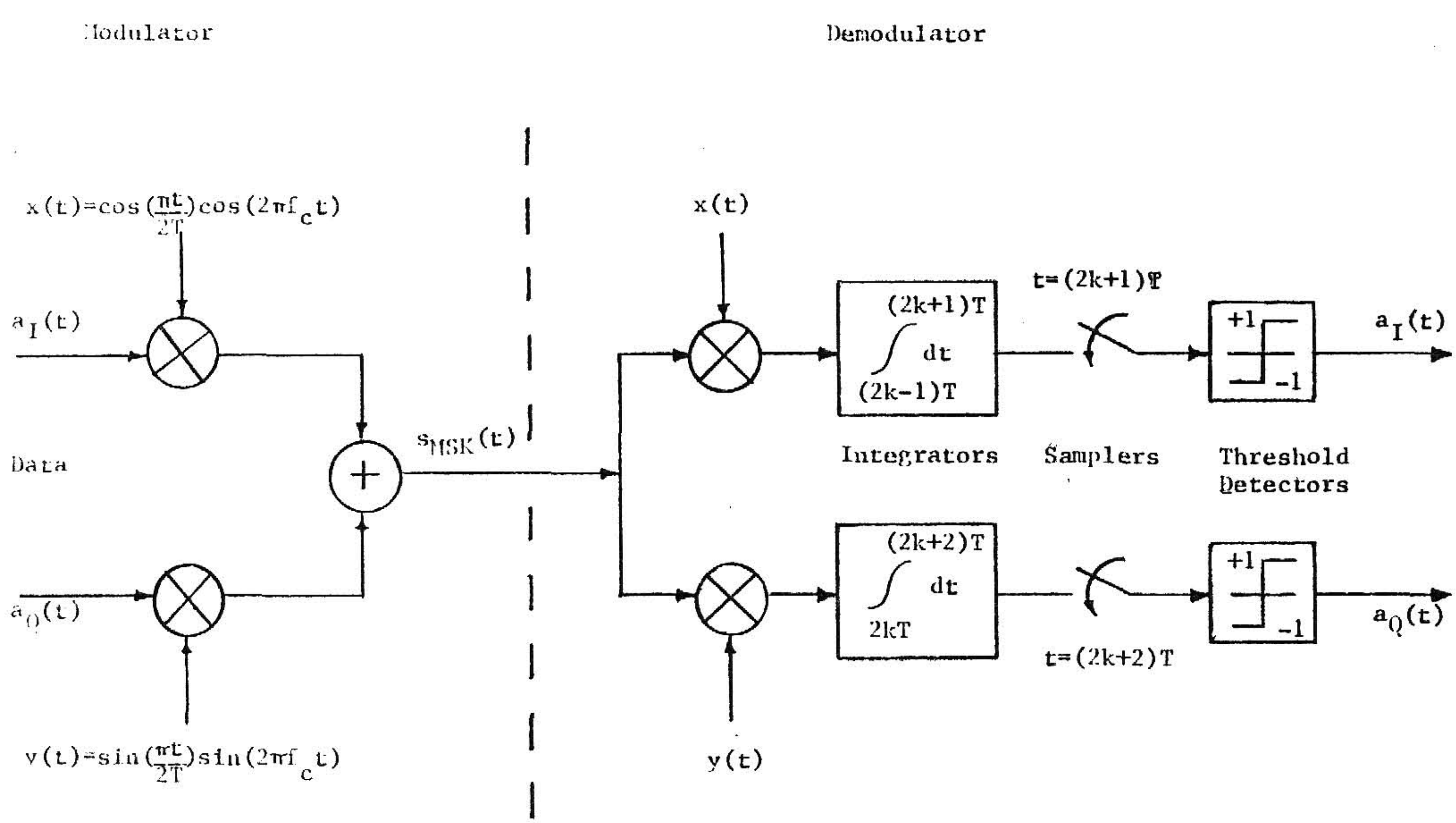

Figure 3. Typical MSK Communication System

I and D circuits and the samplers in their respective channel are offset by T seconds.

Serial Generation of MSK

A serial technique for generating MSK was first given by Amoroso and Kivett [3]. Their approach is shown in Figure 4. Previously it was shown that the MSK signal could be thought of as the sum of two antipodal pulse streams modulating the in-phase and quadrature channels of a single carrier. An alternative approach to modeling MSK given in Figure 3 is to generate the signal by inputing the data serially into a simple BPSK modulator followed by the appropriate bandpass filter. Then the basic data pulse for any integer n is given by

$$p(t) = \frac{T}{\pi}\left\{\frac{2n+2}{2n+1}\right\} \mathrm{SIN}\,\pi\,\frac{t}{2T}\,\mathrm{SIN}\left[\frac{(2n+1)}{2T}\,\pi t + \phi\right], \quad \text{for } 0 \le t \le 2T,$$

$$= 0 \qquad , \text{elsewhere.}$$

It is shown in [3] that a sequence of overlapping transmissions of this form, separated by T second intervals, yields the MSK signal.

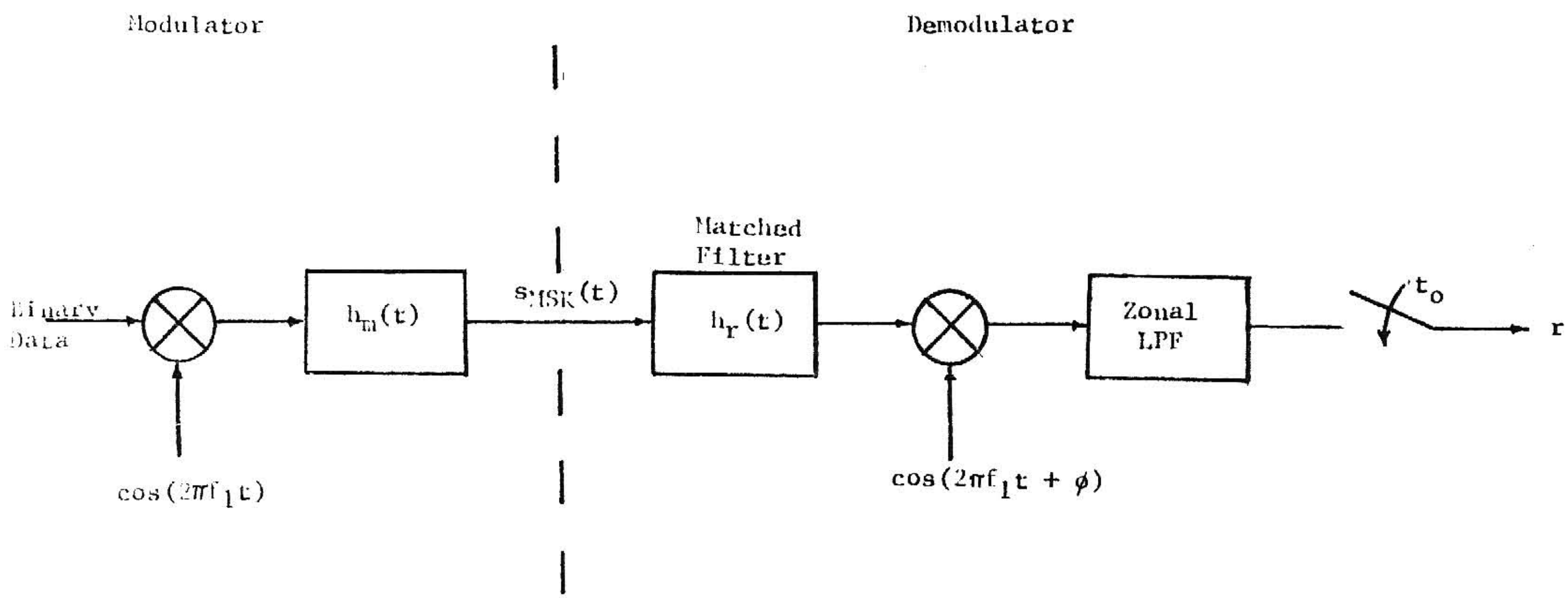

Figure 4. SMSK Communication System

III. MSK FILTER REQUIREMENTS

The input to the ideal SMSK filter $h_m(t)$ (Figure 4), is a simple BPSK signal. The BPSK modulator operates at frequency f_1. The impulse response of the filter is given by

$$h_m(t) = \mathrm{SIN}\ (2\pi f_2 t) \quad , \text{ for } 0 \leq t \leq T, \text{ and}$$
$$= 0 \qquad , \text{ elsewhere} \tag{1}$$

Note that the frequency response of this filter is centered on f_2. The convolution of this impulse response with the BPSK signal yields the desired MSK transmitted signal s(t).

Although the filter response given in (1) is mathematically realizable, a practical implementation is still difficult to achieve. The major objective of the work described here was to determine whether the design of this filter was critical with respect to system performance. The approach taken was to substitute simple filters with similar properties, again centered on f_2 for the ideal MSK filter, and evaluate several performance indicators. It was not known how critical the design of these filters would be so the filter parameters were adjusted until best performance was achieved. The results of the performance evaluation are given in section V.

It is evident that an advantage of SMSK relative to parallel generated MSK is that the modulator is quite simple to construct if the filter synthesis problem can be resolved. The demodulator also is simpler for SMSK. It consists of a prediction matched filter followed by a BPSK demodulator. A zonal low-pass filter at the output produces the desired baseband signal.

IV. COMPUTATIONAL METHODS FOR EVALUATING THE PERFORMANCE OF DIGITAL COMMUNICATION SYSTEMS

An Equivalent Low-Pass Representation

The sub-optimum filters discussed in this paper were evaluated using an equivalent low-pass mathematical model of an SMSK digital communication system. The following development is essentially that of reference [4] which addresses the topic of low-pass modeling of digital systems. This model is well suited for computer analysis. The low-pass representation for a communication system is shown in Figure 5.

The equivalent low-pass representations of filters and signals are needed to develop this model. A bandpass filter with impulse response h(t) has an equivalent low-pass impulse response $\tilde{h}(t)$ which satisfies [5]

$$h(t) = 2 \operatorname{Re} \left\{ \tilde{h}(t)\, e^{jw_c t} \right\} , \tag{2}$$

and a bandpass signal s(t) has an equivalent low-pass representation $\tilde{s}(t)$ which satisfies

$$s(t) = \operatorname{Re} \left\{ \tilde{s}(t)\, e^{jw_c t} \right\} . \tag{3}$$

The equivalent low-pass representation of the transmitted signal s(t) is developed in the following way. Assume that s(t) is a sequence of transmissions given by

$$s(t) = \sum_{n=-\infty}^{\infty} s_n(t-nT_s) \tag{4}$$

where the $n^{\underline{th}}$ transmission $s_n(t)$ is taken from the signal set in accordance with the modulation scheme. Each transmission can be expressed in terms of its complex envelope as

$$\begin{aligned} s_n(t-nTs) &= \operatorname{Re} \left\{ \tilde{s}_n(t-nT_s) e^{jw_c(t-nT_s)} \right\} , \\ &= \operatorname{Re} \left\{ \tilde{s}_n(t-nT_s)\, e^{-jw_c nT_s} e^{jw_c t} \right\} . \end{aligned} \tag{5}$$

This allows the signal to be written as

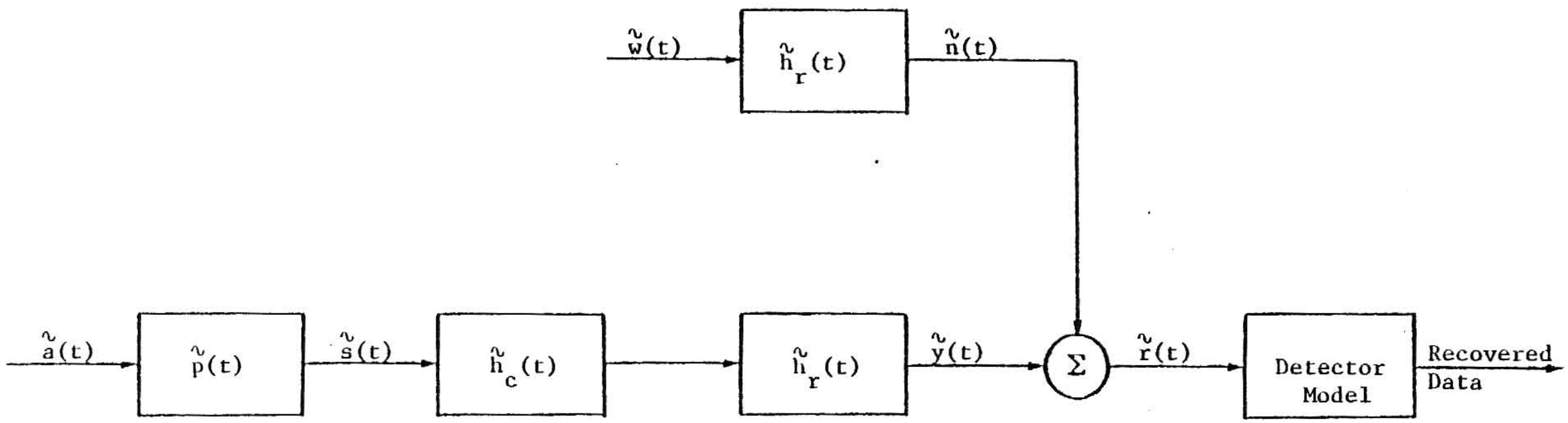

Figure 5. Equivalent Low-Pass Model of a Communication System

$$s(t) = \sum_{n=-\infty}^{\infty} \mathrm{Re}\left\{\tilde{s}_n(t-nT_s)e^{-jw_c nT_s}e^{jw_c t}\right\}$$

or equivalently

$$s(t) = \mathrm{Re}\left\{e^{jw_c t}\sum_{n=-\infty}^{\infty} \tilde{s}_n(t-nT_s)e^{-jw_c nT_s}\right\} . \tag{6}$$

It is clear from [5] that the complex envelope of s(t) is given by

$$s(t) = \sum_{n=-\infty}^{\infty} \tilde{s}_n(t-nT_s)\ e^{-jw_c nT_s} . \tag{7}$$

For many RF modulation schemes, only the amplitude and phase of the signal change from transmission to transmission and the pulse shaping remains the same. Let $\tilde{s}_i(t)$ be represented accordingly as

$$\tilde{s}_i(t) = A_i e^{j\theta_i}\ \tilde{p}(t) \tag{8}$$

where A_i and θ_i are random amplitude and phase symbols corresponding to the message sequence. Substitution into (7) yields

$$\tilde{s}(t) = \sum_{n=-\infty}^{\infty} A_h\ e^{j\theta_n}\ \tilde{p}(t-nT_s)e^{-jw_c nT_s} . \tag{9}$$

Equation (9) is the form used to evaluate the transmitted MSK signal and, with the proper pulse shaping function, can be used to represent BPSK, QPSK, and OQPSK. If $\tilde{p}(t)$ is the impulse response of an equivalent low-pass filter, then $\tilde{s}(t)$ is the output produced by the input sequence of impulses

$$a(t) = \sum_{n=-\infty}^{\infty} A_n e^{j\theta_n} e^{jw_c nT_s}\delta(t-nT_s). \tag{10}$$

The pulse shaping function p(t) is determined by first considering the model given by Amoroso and Kivett for generation of SMSK. Figure 6a shows a coherent BPSK system followed by a bandpass filter. The intermediate low-pass version of this system is shown in Figure 6b.

Development of the Low-Pass Pulse Shaping Function

The BPSK modulator is now modeled by the low-pass pulse shaping function given by the expression

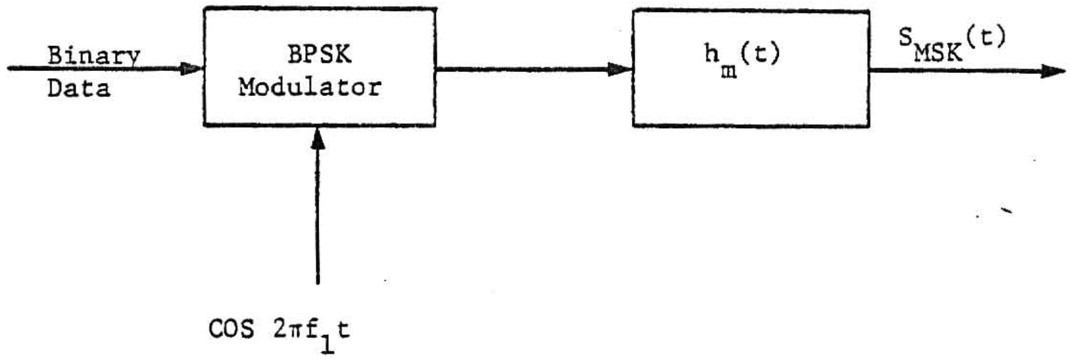

Figure 6a. Model for MSK Generation due to Amoroso and Kivett

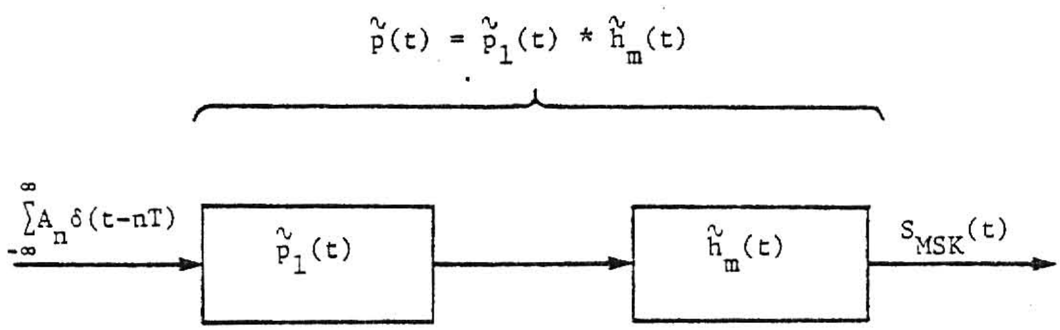

Figure 6b. Intermediate Low-Pass Model for MSK Generation

$$\tilde{p}_1(t) = Ae^{-j\Delta wt} \quad , \quad 0 \leq t \leq T,$$
$$= 0 \quad , \quad \text{elsewhere} \tag{11}$$

where $\Delta w = w_c - w_1$.

The bandpass filter in the MSK modulator is required to have an impulse response

$$h_m(t) = \text{SIN } 2\pi f_2 t \quad , \quad 0 \leq t \leq T,$$
$$= \quad 0 \quad , \quad \text{elsewhere,} \tag{12}$$

and the equivalent low-pass representation of $h_m(t)$ is given by

$$\tilde{h}_m(t) = \frac{1}{2}\, e^{\,j\pi/2}\, e^{j2\pi\Delta ft}, \quad 0 \leq t \leq T,$$
$$= \quad 0 \quad , \quad \text{elsewhere.} \tag{13}$$

The low-pass representation for Amorosso and Kivett's transmitter pulse shaping function model is therefore given by

$$\tilde{p}(t) = \tilde{p}_1(t) \; * \; \tilde{h}_m(t)$$
$$= -j(A/2\Delta w)\text{SIN}\Delta wt \quad , \quad 0 \leq t \leq 2T,$$
$$= \quad 0 \quad , \quad \text{elsewhere.}$$

Note that the SMSK data transmissions occur every T seconds but the signal waveforms last 2T seconds. The pulse shaping function just derived is the form for ideal MSK. Note that the pulse shaping function corresponding to a system which uses a sub-optimum filter is readily obtained by making the appropriate substitution for $h_m(t)$.

Calculation of Power Spectra

The power spectrum of the complex envelope $\tilde{s}(t)$ is found by multiplying the power spectrum, $S_{\tilde{a}}(f)$, of the random data impulse sequence by $|\tilde{P}(f)|^2$ where $\tilde{P}(f)$ is the Fourier transform of $\tilde{p}(t)$. It is a routine exercise to show $S_{\tilde{a}}(f)$ is given by

$$S_{\tilde{a}}(f) = \frac{1}{MT_s} \sum_{i=1}^{M} A_i^2 \triangleq \frac{A_i^2}{T_s} \tag{14}$$

so that the power spectrum of $\tilde{s}(t)$ is thus

$$S_{\tilde{s}}(f) = \frac{\overline{A_i^2}}{T_s} |\tilde{P}(f)|^2 \quad . \tag{15}$$

For SMSK, $\tilde{p}(t)$ is transformed and given by

$$P(f) = \frac{A \text{ COS } (2\pi fT)}{4\pi^2(f^2 - \Delta f^2)} \; e^{-j2\pi fT} \; e^{j\pi/2} \quad . \tag{16}$$

Substitution into (15) gives the equivalent low-pass power spectrum of the SMSK signal as

$$S_{\tilde{s}}(f) = \frac{A^2 \pi \text{COS}^2(2\pi ft)}{16T\pi^2(f^2 - \Delta f^2)^2} \quad . \tag{17}$$

The power spectrum of the bandpass signal s(t) is then found using [5] and given by

$$S_s(f) = 1/4 \; [S_{\tilde{s}}(f-f_c)+S_{\tilde{s}}(-f-f_c)] \quad . \tag{18}$$

The computer programs written to implement the system model of section IV provide the information necessary to calculate $\tilde{P}(f)$ needed by (15). The pulse shaping function $\tilde{p}(t)$ can be expanded in a Fourier series. The coefficients of the expansion are given by

$$c_m = \frac{1}{KT_S} \int_0^{Td} \tilde{p}(t) \; e^{-jm2\pi f_o t} \; dt \tag{19}$$

where
$$f_o = \frac{1}{KT_s} \quad . \tag{20}$$

The Fourier transform of $\tilde{p}(t)$ is

$$\tilde{P}(f) = \int_0^{Td} \tilde{p}(t) \; e^{-j2\pi ft} \; dt. \tag{21}$$

A comparison of (19) and (21) shows that

$$\tilde{P}(mf_o) = KT_s c_m \; . \tag{22}$$

Substitution of (20) and (22) into (15) yields

$$S_{\tilde{s}}\left(\frac{m}{KT_s}\right) = \overline{A_i^2} \; K^2 T_s |C_m|^2 \quad . \tag{23}$$

The calculation of power spectra is not limited to the transmitter output as implied by (23). A more general interpretation would be that $\tilde{P}(f)$ in (15) is the transfer function of two or more filters in cascade. For example, the power spectrum of the signal entering the detector would be

$$S_{\tilde{r}}\left(\frac{m}{KT_s}\right) = \overline{A_i^2}\, K^2 T_s \left| C_m \tilde{H}_c(m2\pi f_o)\, \tilde{H}_r(m^2 2\pi f_o)\right|^2 \quad . \tag{24}$$

Detection

The detector used in the analysis consists of a product detector followed by a zonal low-pass filter and a sampler as shown in Figure 7. The detector reference is at frequency w_r rad/sec. For most analytical work it is convenient to include any matched filter or other receiver filters as part of $h_r(t)$ so that the only purpose of the zonal low-pass filter is to eliminate sum frequency terms generated by the detector. The sampler operates at the signaling rate. It is assumed that the sample of interest, r, is taken at instant t_o. An expression for r is readily obtained by noting that it is found as the low-pass part of

$$e_d(t) = r(t) \cos(w_1 t + \emptyset) \; . \tag{25}$$

In terms of complex envelopes, $e_d(t)$ is given by

$$e_d(t) = \mathrm{Re}\left\{\tilde{r}(t)\, e^{jw_c t}\right\} \cos(w_1 t + \emptyset)$$

$$= \frac{\tilde{r}(t) e^{jw_c t} + \tilde{r}^*(t)\, e^{-jw_c t}}{2} \cdot \frac{e^{j(w_1 t + \emptyset)} + e^{-j(w_1 t+\emptyset)}}{2} \; .$$

Carrying out the indicated multiplication and discarding sum frequency terms yields

$$\underset{\text{(low-pass terms)}}{e_d(t)} = 1/4\left\{\tilde{r}(t) e^{j[(w_c - w_1)t - \emptyset]} + \tilde{r}^*(t) e^{-j[(w_c - w_1)t - \emptyset]}\right\} . \tag{26}$$

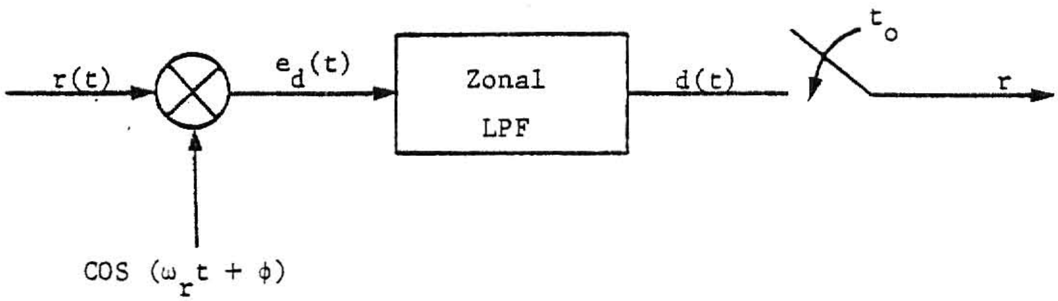

Figure 7. Detector Model

The sample r is therefore given by an equivalent form evaluated at $t=t_0$, Viz.,

$$r = \frac{1}{2}\,\mathrm{Re}\{\tilde{r}(t_0)\, e^{-j\phi} e^{j(w_c-w_1)t_0}\} \quad . \tag{27}$$

Note that w_1 is the mark frequency in radians per second.

Matched Filter Receiver

In this communication system, a matched filter was used at the front end of the receiver. For analysis purposes, it is convenient to include the matched filter as part of the impulse response $h_r(t)$. An equivalent low-pass representation for the matched filter is readily obtained by recalling that the impulse response of a filter matched to the signal $s_i(t)$ is

$$h_r(t) = s_i(T_d-t), \tag{28}$$

where T_d is the duration of the signal. Using the complex envelope representation for $s_i(t)$ yields

$$\begin{aligned} h_r(t) &= \mathrm{Re}\{\tilde{s}_i(T_d-t)e^{jw_c(T_d-t)}\} \\ &= \mathrm{Re}\{\tilde{s}_i^*(T_d-t)e^{-jw_cT_d}\, e^{jw_ct}\} \ . \end{aligned} \tag{29}$$

Taking (29) together with the requirement that $h_r(t)$ satisfy (2) leads to

$$\tilde{h}_r(t) = \frac{1}{2}\,\tilde{s}_i^*(T_d-t)e^{-jw_cT_d} \tag{30}$$

as the equivalent low-pass representation of the impulse response of the filter matched to $s_i(t)$. A frequency domain representation is sometimes more convenient. Transforming (30) yields $\tilde{H}_r(w)$ as

$$\tilde{H}_r(w) = \frac{1}{2}\,\tilde{S}_i^*(w)e^{-jw_cT_d}\, e^{-jwT_d} \quad . \tag{31}$$

Error Rate Calculations

Using the low-pass model of Figure 5, the method used to calculate bit error probability, P[e] is as follows. The expression for $\tilde{s}(t)$ given in equation (9) can be simplified by defining the complex data symbol a_n as

$$a_n = A_n e^{j\theta_n} \quad . \tag{32}$$

Substitution into (9) yields

$$\tilde{s}(t) = \sum_{n=-\infty}^{\infty} a_n e^{-jw_c nTs} \tilde{p}(t-nT_s) \quad . \tag{33}$$

Now expand the pulse shaping function p(t) in a Fourier series using a periodic extension of $\tilde{p}(t)$ having a period somewhat longer than the effective memory of the channel receiver filters. For convenience it is required that the period be a multiple of the bit time, i.e., let P=kT where k is an integer selected such that kT is greater than the effective duration of the receiving system response $\tilde{h}_r(t)$. Then over the time interval of interest a good approximation for $\tilde{p}(t)$ is

$$\tilde{p}(t) \approx \sum_{m=-\infty}^{\infty} c_m e^{jmw_o t} \tag{34}$$

where c_m is the Fourier coefficient and $w_o = 2\pi/kT$.
Using this series approximation in (33) yields

$$\tilde{s}(t) = \sum_{n=-\infty}^{\infty} \sum_{m=-\infty}^{\infty} a_n c_m e^{-jnw_c T_s} e^{-jnmw_o T_s} e^{jmw_o t} \quad . \tag{35}$$

The signal portion, $\tilde{y}(t)$, of the received complex envelope, r(t), is found by convolving $\tilde{s}(t)$ with $\tilde{h}_r(t)$, i.e.,

$$\tilde{y}(t) = \int_{-\infty}^{\infty} \tilde{h}_r(t-\tau) \sum_{n=-\infty}^{\infty} a_n c_m e^{-jnw_c T_s} e^{-jnmw_c T_s} e^{jmw_o \tau} d\tau \quad . \tag{36}$$

Interchanging the order of integration and summation yields

$$\tilde{y}(t) = \sum_{n=-\infty}^{\infty} \sum_{m=-\infty}^{\infty} a_n c_m e^{-jnw_c T_s} e^{-jnmw_c T_s} \int_{\infty}^{\infty} \tilde{h}_r(t-\tau) e^{jmw_o \tau} d\tau \quad . \qquad (37)$$

By making the change of variables $u=t-\tau$, the integral in (37) becomes

$$\int_{-\infty}^{\infty} h_r(u)\, e^{-jmw_o u}\, du\; e^{jmw_o t} = \tilde{H}_r(mw_o) e^{jmw_o t} \quad ,$$

thus the preceding reduces to

$$\tilde{y}(t) = \sum_{n=-\infty}^{\infty} \sum_{m=-\infty}^{\infty} a_n c_m \tilde{H}_r(mw_o) e^{-jnw_c T_s} e^{-jnmw_o T_s} e^{jmw_o t} \quad . \qquad (38)$$

This equation is ideal for evaluation with the exception of the infinite sums. For practical purposes, it is reasonable to truncate both summations. Any real transmitter has an assigned channel bandwidth, therefore the Fourier series expansion of $\tilde{p}(t)$ can be restricted accordingly. The transmission series can also be truncated since only a few transmissions contribute to $\tilde{y}(t)$ unless the system has a very long memory. In the computer analysis, the transmission of interest corresponds to n=o. The index n is restricted to the range (-N,1) where N is a positive integer such that NT_s exceeds the effective duration of $\tilde{h}(t)$. The transmission for n=o is included because this "future" transmission can interfere with the decision on the symbol sent at t=o. The resulting expression for $\tilde{y}(t)$ valid for $o \leq t \leq 2T_s$ is

$$\tilde{y}(t) = \sum_{n=-N}^{1} \sum_{m=-M}^{M} a_n c_m \tilde{H}_r(mw_o) e^{-jnw_c T_s} e^{-jnmw_o T_s} e^{jmw_o t} \quad . \qquad (39)$$

The complex envelope of the received signal is the sum of this signal term and a noise term, i.e.,

$$\tilde{r}(t) = \tilde{y}(t) + \tilde{n}(t) \qquad (40)$$

where $\tilde{n}(t)$ is the low-pass representation of the noise signal n(t) produced by Gaussian white noise at the receiver input. The rest of the probability of error development can be found in [4].

Eyepattern Development

An eyepattern is a graph of all possible output waveform sequences superimposed on each other over one signaling interval. It is desired to only look at the data signal portion of the received signal. The noise, n(t), is thus set to zero in equation 40. The output waveform can be found by substituting (40) into (27) and replacing the sampling instant t_o by the continuous variable t yielding

$$d(t) = \frac{1}{2} \mathrm{Re}\{\tilde{y}(t)e^{-j\phi} e^{j(w_c - w_1)t}\} \quad . \tag{41}$$

The eyepattern plots in the following sections show the effect of intersymbol interference on the output waveform which is caused by the filters memory.

Signal Envelope Development

The envelope of the signal can be found by realizing that the equivalent low-pass representation of the transmitted signal, y(t), is a description of the signals complex envelope. The envelope is usually expressed in terms of magnitude and phase. The magnitude of the signal envelope is

$$|\tilde{y}(t)| = \mathrm{SQRT}\ [|\tilde{y}(t)|^2], \tag{42}$$

and the phase is given by

$$\mathrm{ARG}\{\tilde{y}(t)\} = \mathrm{TAN}^{-1}\left|\frac{\mathrm{Im}\{\tilde{y}(t)\}}{\mathrm{Re}\{\tilde{y}(t)\}}\right| \quad . \tag{43}$$

By observing different data sequences of the set $(A_n e^{j\theta_n})_{n=-N}^{1}$ it can be seen how the complex envelope will react.

All of the results in the following analysis of the two suboptimum systems were obtained on a minicomputer operating with 32k of core memory. Execution times were generally between one to three minutes.

V. SUBOPTIMUM SMSK MODULATION

Two simple filter configurations are now considered as alternatives to the ideal SMSK filter given in (12). The pulse shaping function p(t) will be modeled as previously given in Figure 6b. The ideal impulse response $\tilde{h}_m(t)$ will be replaced first by that of a simple four-pole Butterworth filter and its system will be referred to hereafter as the SMSK-Butterworth system. The second configuration consists of a four-pole Butterworth followed by a double-notch filter. The impulse responses of these filters are convolved to yield $\tilde{h}_m(t)$ for this case. This system is designated as the SMSK-Stub Butterworth system.

SMSK-Butterworth

The first step in evaluating the performance of the SMSK-Butterworth system is determination of $\tilde{H}_m(w)$ which in this case is a Butterworth form. The transfer function of a Butterworth filter is

$$\tilde{H}_B(s) = \frac{Ho}{B_n(s)} \tag{44}$$

where Ho is the gain of the filter and $B_n(s)$ is the Butterworth polynomial of order n. If $B_n^{\prime}(s)$ is a normalized (tables of normalized polynomials to one rad/sec cut-off frequency are widely available) polynomial with w_o the desired cut-off frequency, then

$$\tilde{H}_B(s) = \frac{Ho}{B_n^{\prime}(s/w_o)} \quad . \tag{45}$$

The rest of the discussion will be concerned with a simple four-pole Butterworth with gain $H_o = 1$. It is well known [8] that the magnitude response of this filter is given by

$$|\tilde{H}_B(w)| = \frac{1}{\sqrt{1+w^{2n}}} \tag{46}$$

where n is equal to the number of poles, in this case four. The argument of a four-pole Butterworth is given by

$$\mathrm{ARG}\{\tilde{H}_B(w)\} = -\mathrm{TAN}^{-1}\left(\frac{a_1 w}{1-w^2}\right) -\mathrm{TAN}^{-1}\left(\frac{a_2 w}{1-w^2}\right) \tag{47}$$

where a_1 and a_2 are the coefficients of the Butterworth for n=4.

The frequency response of the ideal system is now examined to obtain the proper frequency selections for the Butterworth filter. The power spectra of the output of the BPSK modulator $S_{PSK}(t)$, the ideal SMSK filter response, and the ideal SMSK transmitted signal spectrum are shown in Figure 8. Let $f_s = 1/T_s$ be the bit rate. The mark and space frequencies, f_1 and f_2, and the apparent carrier frequency, f_c, are represented by

$$f_1 = \frac{n}{2} f_s \quad ,$$

$$f_2 = \frac{n}{2} f_s + \frac{1}{2} f_s \quad , \text{ and}$$

$$f_c = \frac{n}{2} f_s + \frac{1}{4} f_s \tag{48}$$

where n is a positive integer.

The upper and lower nulls of the SMSK signal spectrum are readily determined to be

$$f_{un} = n/2f_s + f_s \quad \text{and}$$
$$f_{ln} = n/2f_s - \frac{1}{2} f_s . \tag{49}$$

As can be seen from Figure 8, the four-pole Butterworth should be centered on f_2 or off-set relative to f_c by $\Delta f = f_2 - f_c = \frac{1}{4T_s}$.

The cut-off frequencies for the Butterworth filter was determined using the 3dB bandwidth criterion. Figure 8 shows the SMSK power spectrum with cut-off frequencies f_{cu} and f_{cl} where the 3dB bandwidth is given by

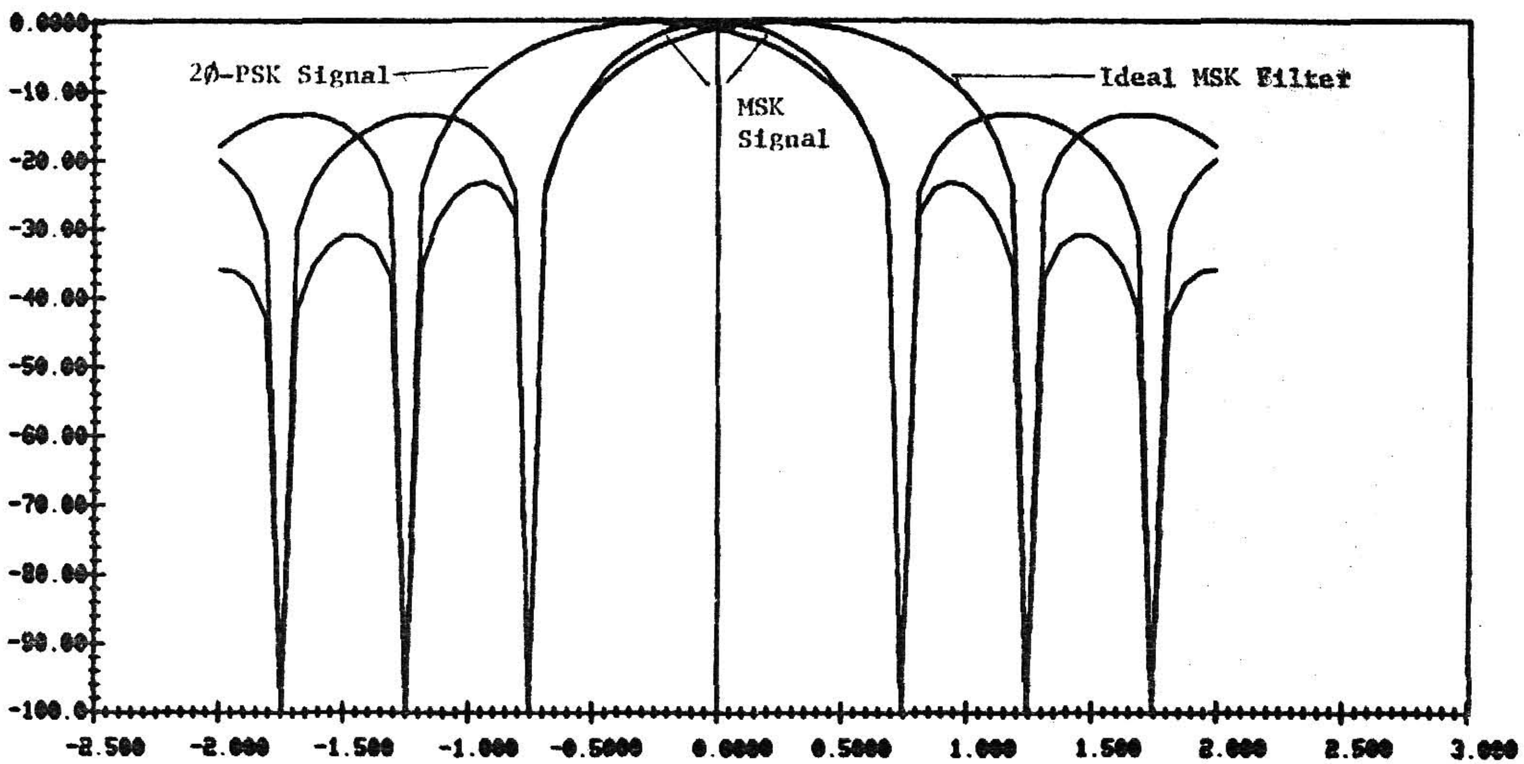

Figure 8. Frequency Response at Different Points in the Transmitter

$$B_{3dB} = f_{cu}-f_{cl} = 2(f_{cu}-f_c). \tag{50}$$

Note that the bandwidth desired is with respect to the low-pass representation of the SMSK signal spectrum centered at f_c and therefore f_c=0 in (50). The expression representing the SMSK signal spectrum is given by

$$S_{MSK}(f) = \frac{SIN(\pi f T_s)}{\pi f T_s} \quad . \tag{51}$$

Setting $S_{MSK}(f_{cu}) = 0.707$ and solving for f_{cu} yields

$$f_{cu} = 0.443/T_s. \tag{52}$$

Substituting (52) into (50) gives

$$B_{3dB} = 2f_{cu} = \frac{0.886}{T_s} \simeq 1/T_s = f_{cut\text{-}off}, \tag{53}$$

for convenience. Included now is the variable R so the bandwidth may be adjusted later if desired. R is the ratio of the 3dB bandwidth (Hz) to the bit rate (bps). The cut-off frequency f_{co} will now be written as

$$f_{cut\text{-}off} = \frac{R}{T_s} \quad .$$

Now, substitute for w in equations (46) and (47), the desired bandpass cut-off frequency w_{co} with the desired translation $\Delta w = 2\pi/4T_s$ gives

$$\hat{f} = \frac{f-\Delta f}{f_{c.o.}} = \frac{f - \frac{1}{4}T_s}{R/T_s} = \frac{fT_s - 0.25}{R} \, . \tag{54}$$

Substituting (54) into (46) yields

$$|\tilde{H}_B(\hat{f})| = \frac{1}{\sqrt{1 + \frac{\overline{(fT_s - 0.25)}}{R}}} \quad . \tag{55}$$

The low-pass Butterworth coefficients a_1 and a_2 for four-pole designs are 0.765 and 1.848 respectively. Substituting the coefficients along with $\hat{f}$ gives

$$\mathrm{ARG}\{\tilde{H}_B(f)\} = -\mathrm{TAN}^{-1}\left[\left(\frac{0.765\ \hat{f}}{1 - \hat{f}^2}\right)\right] - \mathrm{TAN}^{-1}\left[\left(\frac{1.848\ \hat{f}}{1 - \hat{f}^2}\right)\right]$$

where $\hat{f}$ is given by (54).

RESULTS

The data obtained using the Butterworth filter in the modulator instead of the ideal filter showed surprisingly good communication efficiency. Five properties considered in the analysis were:

1) Bit Error Probability
2) Power Spectrum
3) Transmitted Signal Envelope
4) Eyepattern
5) Transmitted Signal

Note that the receiver filter is matched to the transmitter as given in (28). After taking all five properties into consideration it was found that a ratio of R=0.5 yielded the best performance.

The probability of error curve using the Butterworth impulse response with different ratios is shown in Figure 9. It can be seen that the P[e] curve with ratio of R=0.5 comes close to ideal SMSK.

The comparison of the transmitted signal power spectra are shown in Figure 10. The power spectrum was significantly more compact using the Butterworth filter.

The next property considered was the signal envelope. Ideal SMSK has a perfectly flat envelope. Figure 11 shows a comparison of envelopes of the Butterworth filter with different bandwidths and the ideal case. An alternating sequence was used to determine these envelopes. Although not as good as ideal SMSK, the non-ideal envelopes were fairly flat. The ratio was then fixed at R=0.5 and the sequence was varied. It can be seen from Figure 12 that the varied sequence did not degrade the envelope significantly.

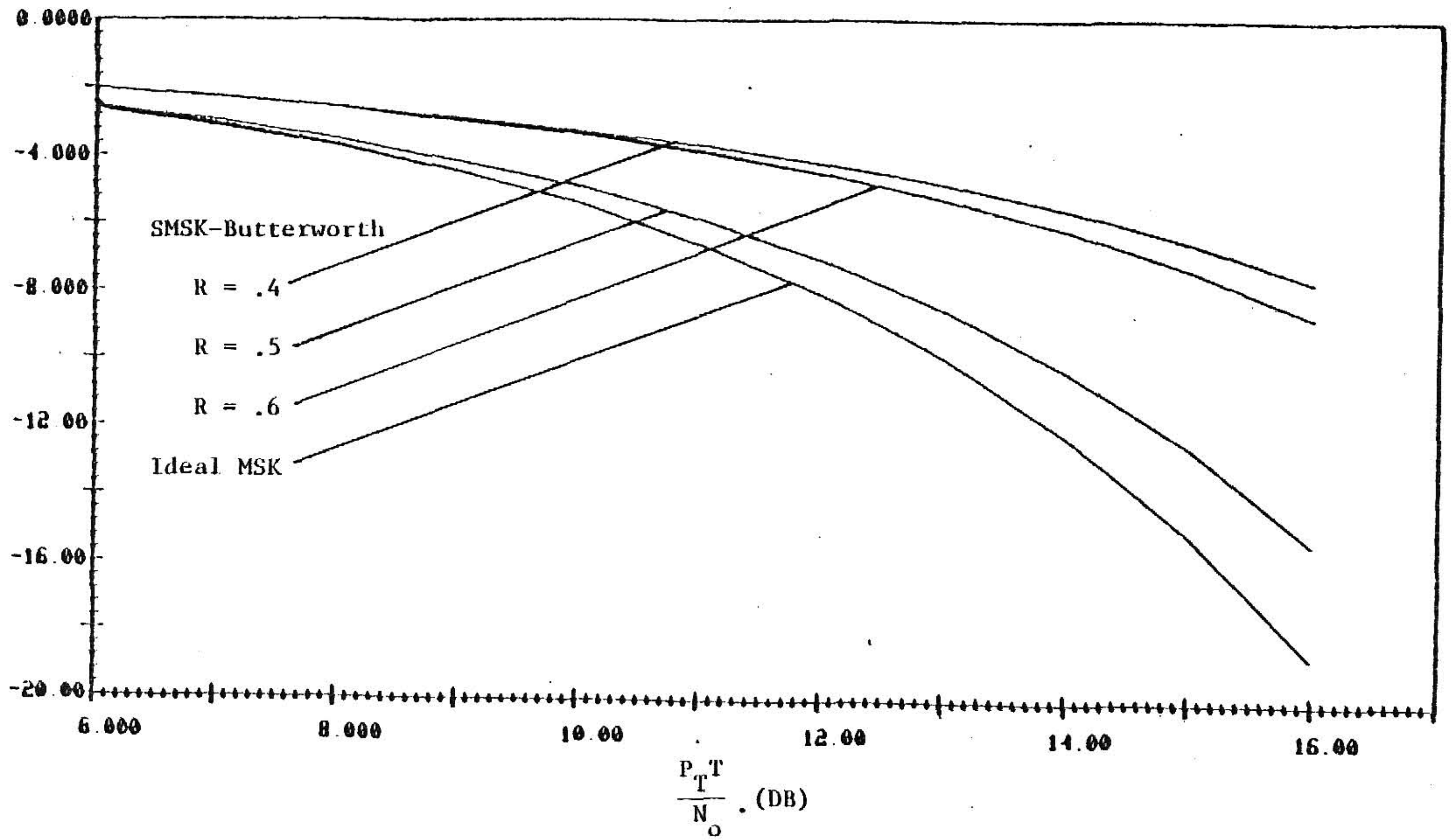

Figure 9. SMSK-Butterworth Error Probability

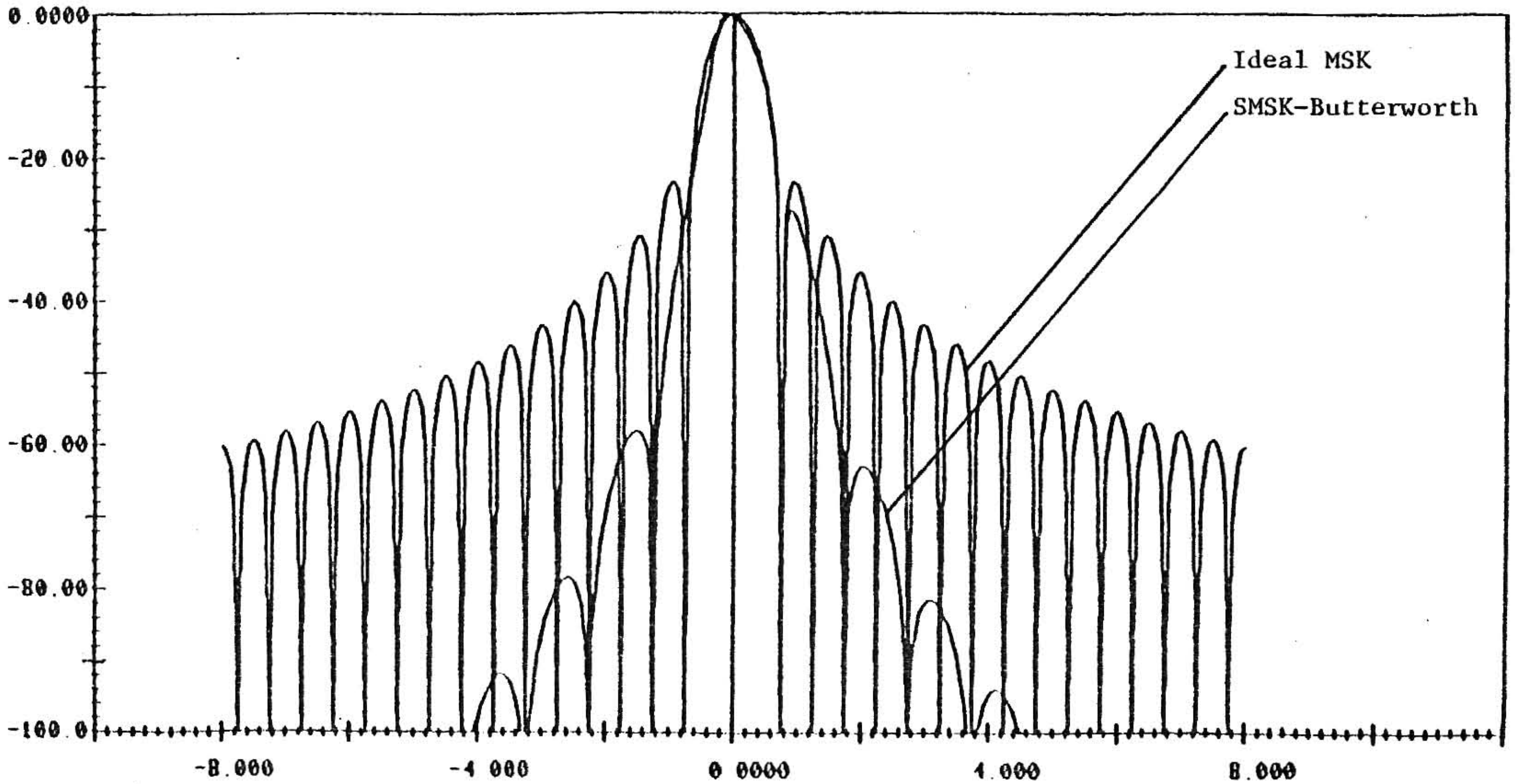

Figure 10. SMSK-Butterworth Normalized Power Spectra

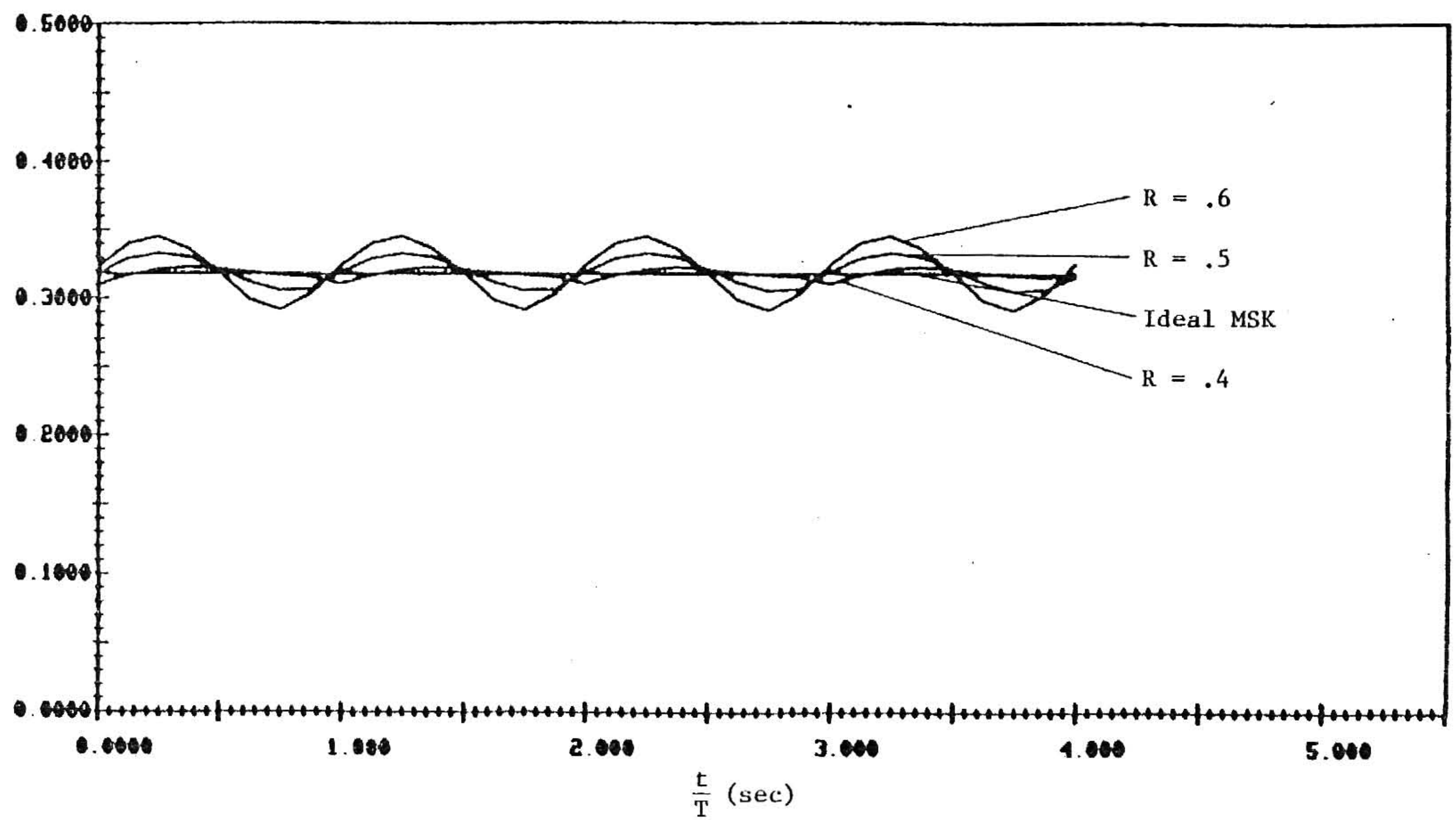

Figure 11. SMSK-Butterworth Signal Envelope, R Varied

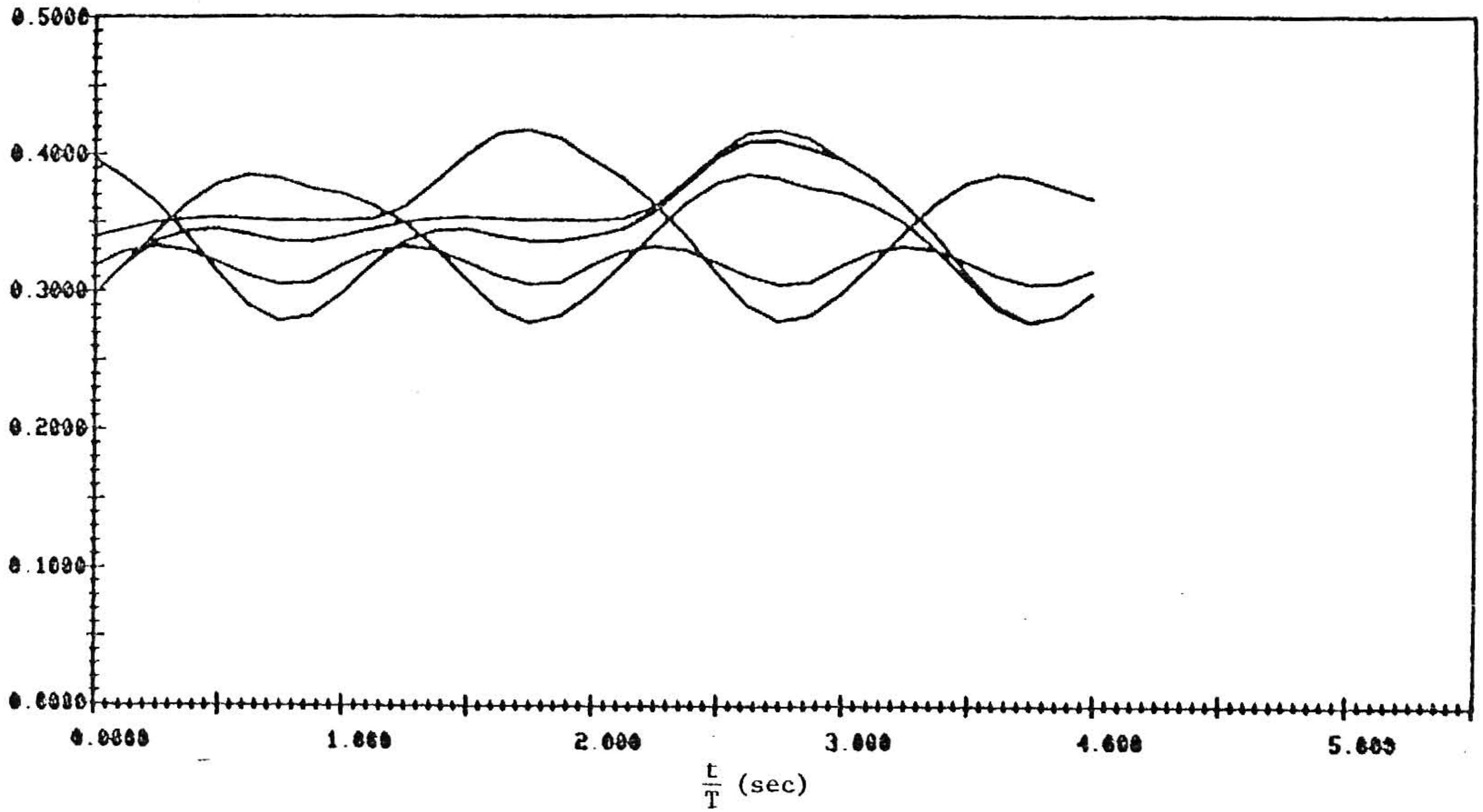

Figure 12. SMSK-Butterworth Signal Envelope, Sequence Varied

Figures 13 through 16 show the eyepatterns using the SMSK Butterworth system, again with different ratios, and the ideal system. Once again the eyepattern with ratio of R=0.5 proved to be the best and came closest to the ideal SMSK system eyepattern.

The last calculation was of the transmitted signal for the case n=2. The ratio was varied again and compared with the ideal case as shown in Figure 17. The sub-optimum system did demonstrate continuity at the bit transitions although the signal was slightly offset.

SUMMARY

The sub-optimum SMSK-Butterworth system demonstrated:

1) Low Probability of Error
2) Very Compact Power Spectrum
3) Reasonably Flat Envelope
4) Open Eyepattern
5) Continuous Signal Phase at the Data Transitions

All properties considered, the Butterworth system approaches the same high communication efficiency as the ideal SMSK system. The only significant weakness is the envelope variation.

SMSK-Stub Butterworth

The SMSK-Stub Butterworth* system is only slightly more complicated than the case just described. The SMSK transmitter is modeled as shown in Figure 18. The impulse response $\tilde{h}_m(t)$ is replaced with the impulse response of a double-notch filter followed by a four-pole Butterworth or

$$\tilde{h}_m(t) = \tilde{h}_s(t) * \tilde{h}_B(t) \quad . \tag{56}$$

The computer programs actually use the transfer function so it is necessary

* This idea was revealed through private communication with C. Ryan, Motorola Communications Systems Research Laboratory, Gilbert, Arizona.

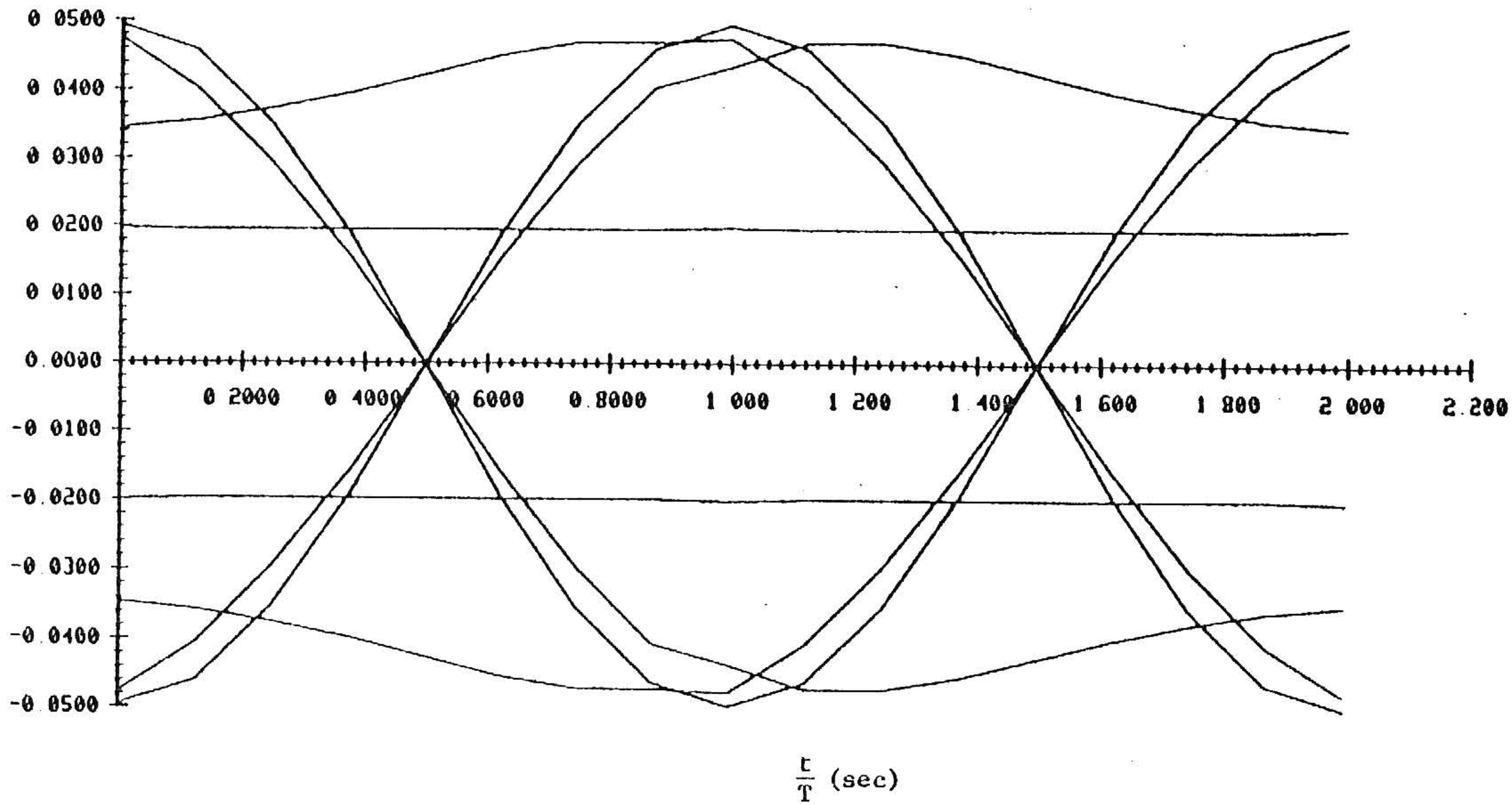

Figure 13. SMSK-Butterworth Eye Pattern, R = .4

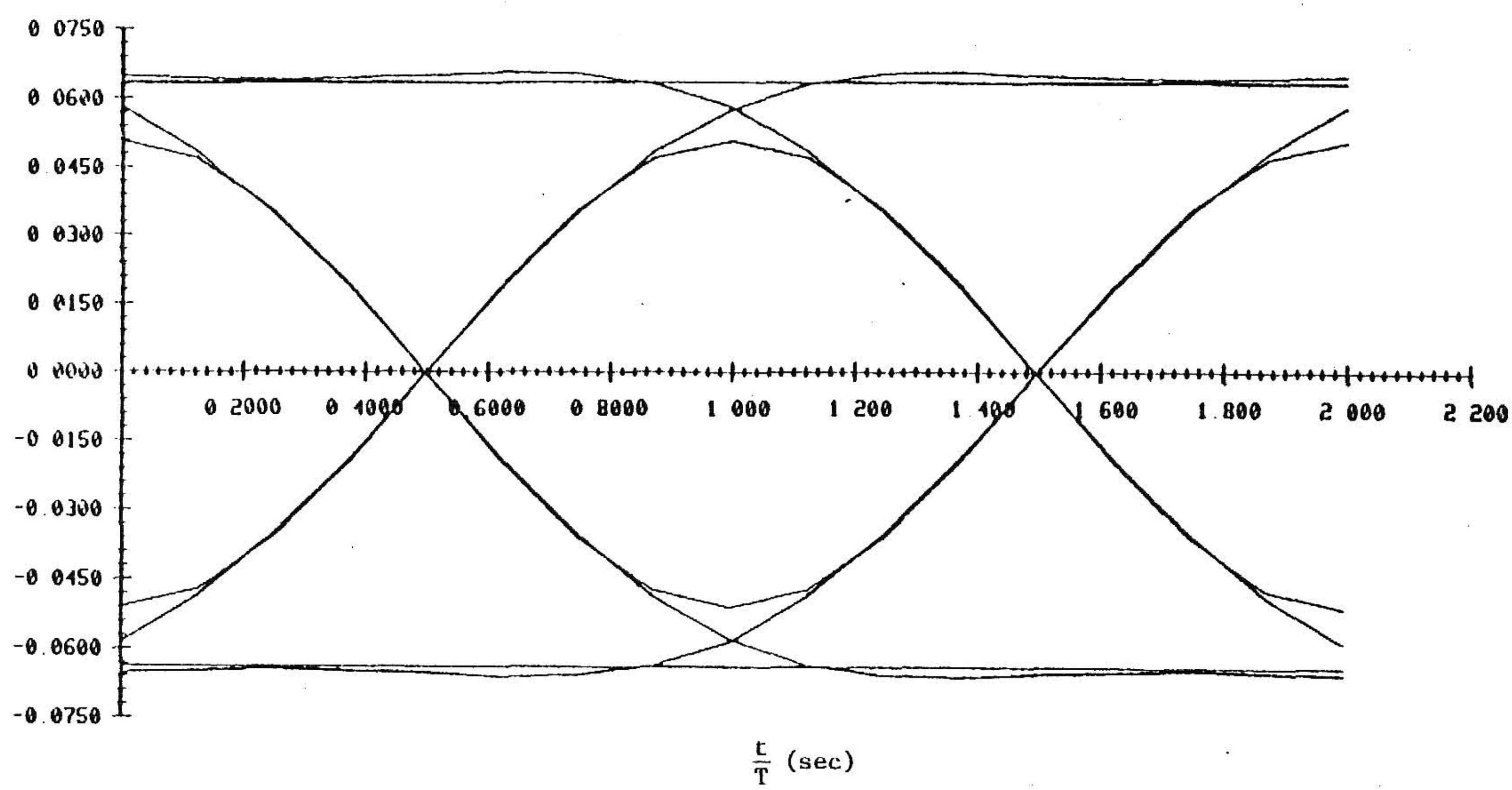

Figure 14. SMSK-Butterworth Eye Pattern, R = .5

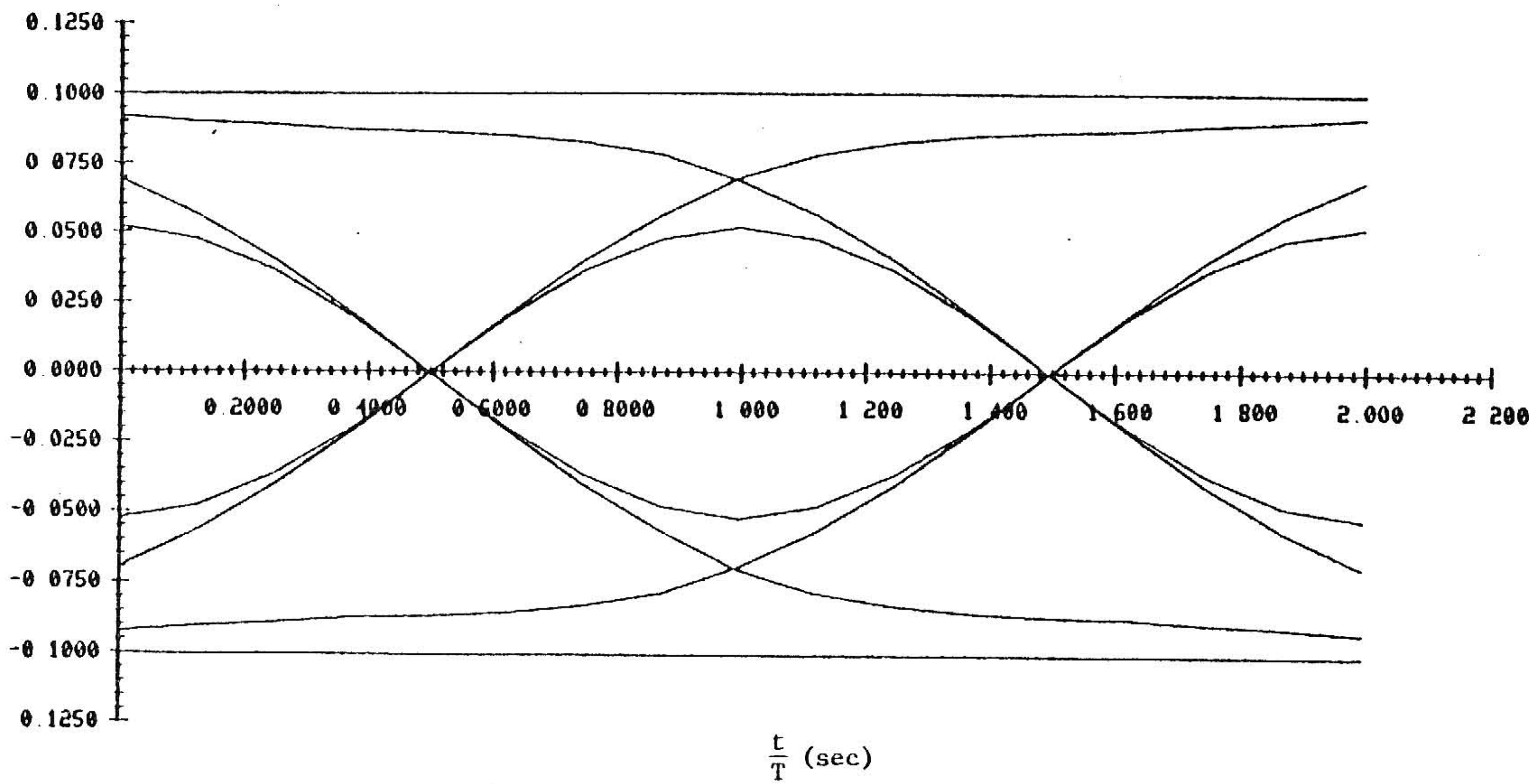

Figure 15. SMSK-Butterworth Eye Pattern, R = .6

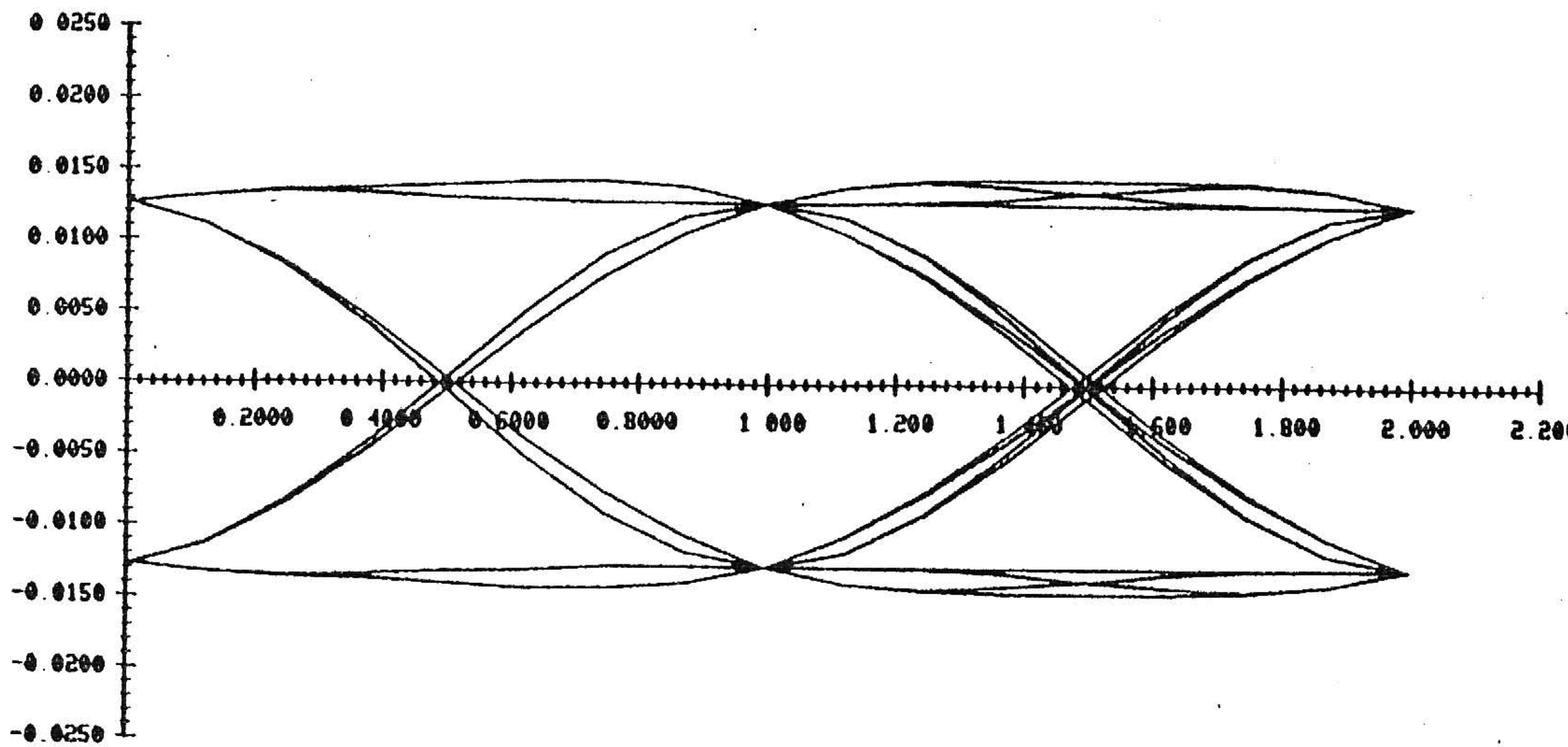

$\frac{t}{T}$ (sec)

Figure 16. Ideal MSK Eye Pattern

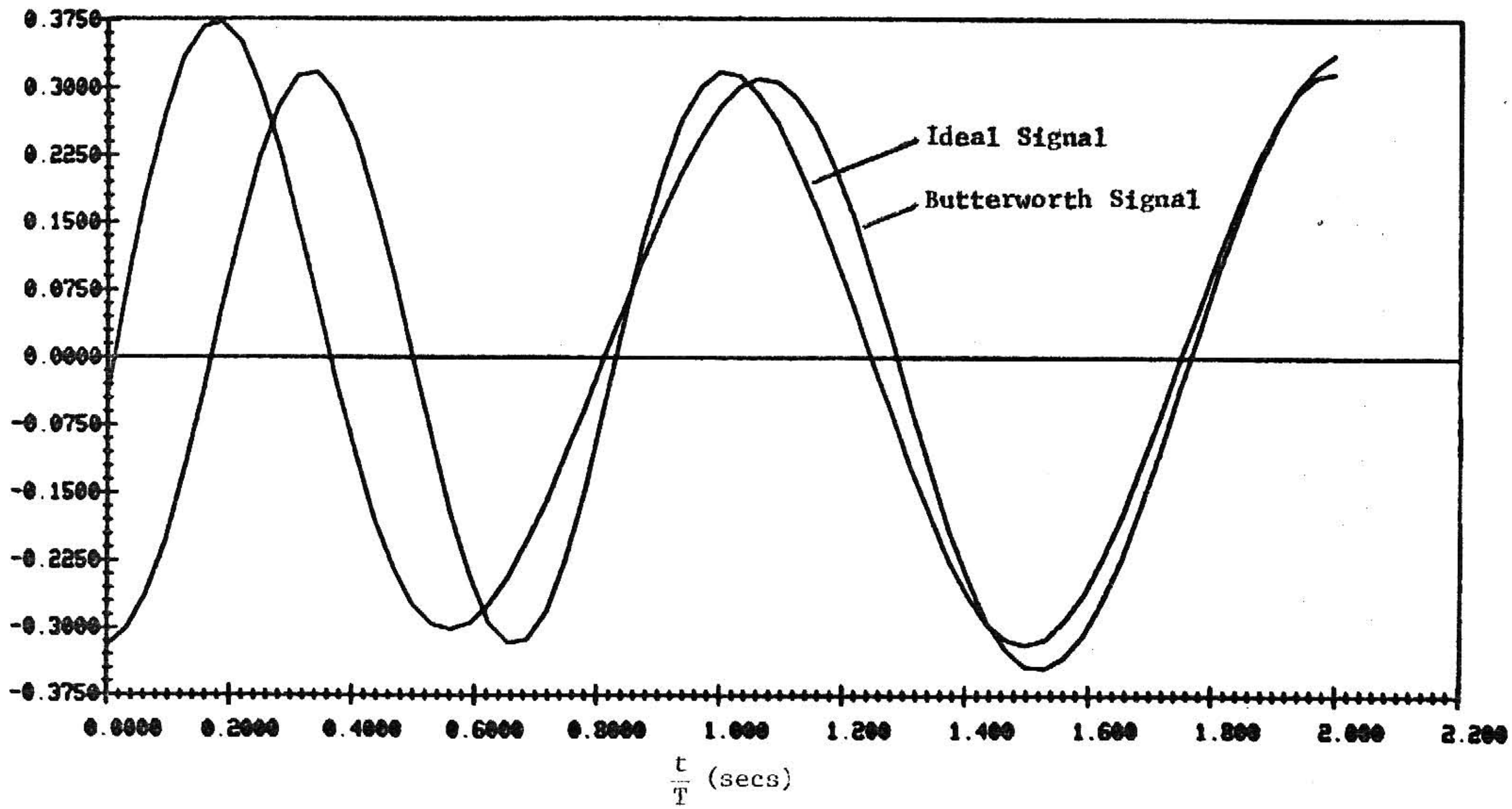

Figure 17. SMSK-Butterworth Transmitted Signal

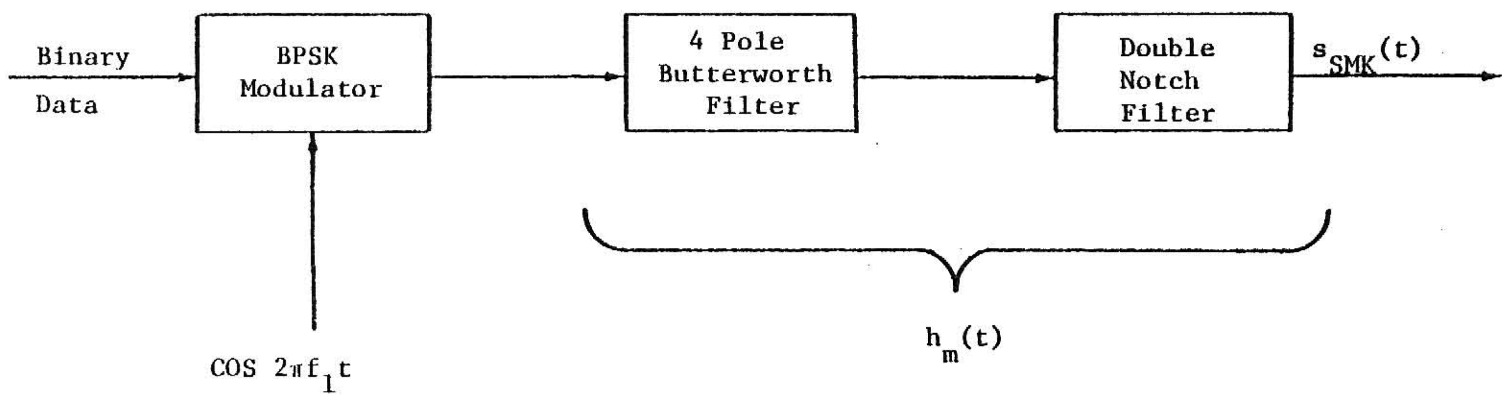

Figure 18. Model for SMSK-Stub Butterworth Generation

to find $\hat{H}_m(f) = \hat{H}_s(f) \cdot \hat{H}_B(f)$. The same Butterworth filter was used in this analysis as in the previous discussion.

The double-notch filter was developed in the following way and can be modeled as shown in Figure 19. The transfer function is given by

$$H_s(f) = \frac{1/Y_T}{1/Y_T + 1/Y_o} = \frac{1}{1 + Y_{T/Y_o}} \tag{57}$$

where Y_T is the equivalent parallel admittance of Y_o, Y_u, and Y_l. Y_u and Y_l represents the upper and lower notch admittances respectively. A notch in the filter is represented by the equation

$$Y_{notch} = jY_o \ \mathrm{TAN}(\beta l). \tag{58}$$

It is desired that the notch impedance short circuit when $f=f_{notch}$, which happens when $\beta l = \pi/2$. The selection of β and l is as follows. β is defined as

$$\beta = 2\pi/\lambda \tag{59}$$

where λ is the wavelength. The parameter l is defined as

$$l = \frac{k\lambda_n}{4} \ , \tag{60}$$

the open stub line length where k is an odd integer. Since

$$\lambda = c/f, \tag{61}$$

where c is the speed of light and f is the frequency. Substitution of (61) into (59) and multiplying by (60) yields

$$\beta l = \frac{k\pi}{2} f/_{fn} \ . \tag{62}$$

The notches are to be located at

$$f_{ln} = f_2 - f_s \text{ and}$$
$$f_{un} = f_2 + f_s \tag{63}$$

where again f_2 is the center frequency of the SMSK filter and $f_s=1/Ts$, the bit rate. These notches were determined by the nulls of the ideal

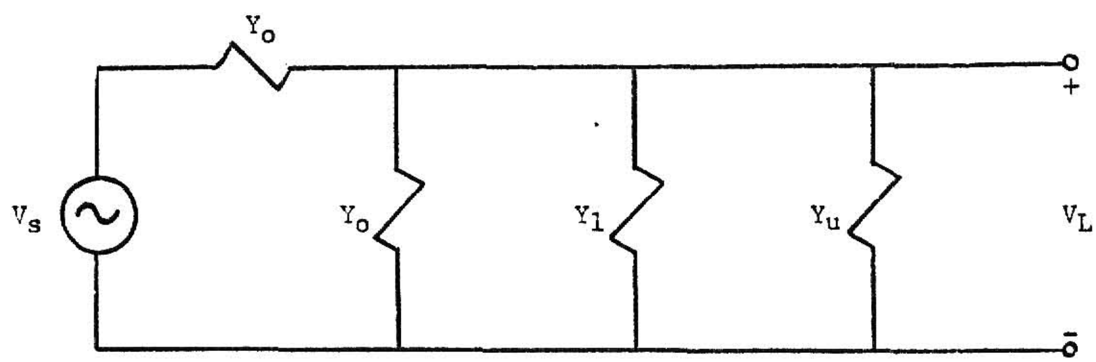

Figure 19. Double-Notch Filter Model

SMSK filter spectrum (Figure 8). Substituting equations (63) into (62), (62) into (58), and (58) into (57) yields

$$H_s(f) = \frac{1}{2 + j(\mathrm{TAN}(\pi/2\ f/f_{1n}) + \mathrm{TAN}(\pi/2\ f/f_{un}))} \quad . \qquad (64)$$

For analysis, the low-pass transfer function is needed. This is given by

$$\tilde{H}_s(f) = H_s(f+fc)$$

where f_c is the apparent carrier frequency of the transmitted signal. Figures 20a and 20b show the notch filter and pulse shaping filter power response.

RESULTS

Evaluation of the SMSK system with the ideal SMSK impulse response replaced by the Stub-Butterworth impulse response reveal improvement over the case of the previous section. When considering the five properties previously discussed, it was found that the best results were obtained when ratio R=0.65 and k=7.

The bit error curves of the SMSK-Stub Butterworth system compared with ideal SMSK is shown in Figure 21. The error curves for k=7 and the ideal case are extremely close.

Figure 22 compares the normalized power spectrum. It can again be seen that the Stub-Butterworth system has a very compact spectrum when compared with ideal SMSK.

The ideal and Stub-Butterworth transmitted signal envelopes are compared in Figure 23. The envelope is nearly flat and approaches the ideal case in all three choices for k.

Figure 24 through 26 show the eyepatterns for the respective choice of k. It can be seen that k=7 yields the cleanest pattern.

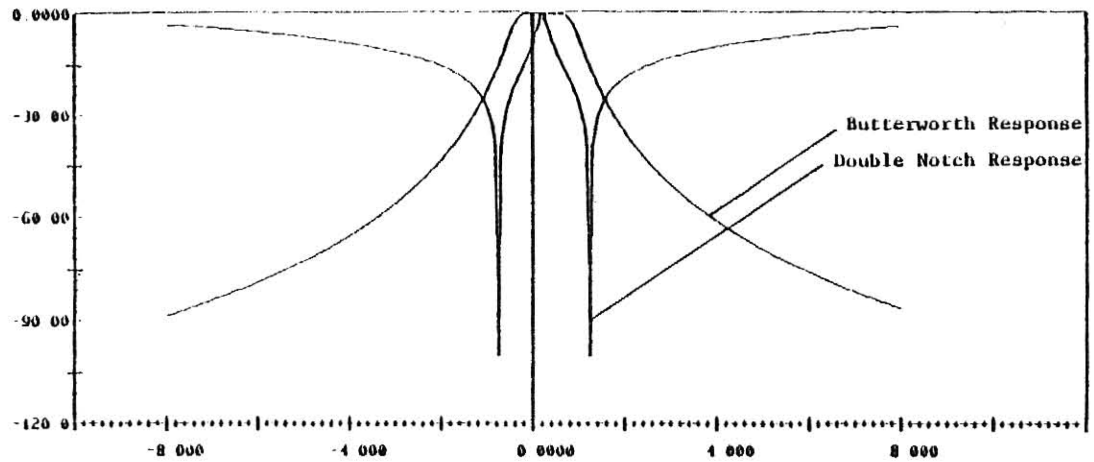

Figure 20a. SMSK-Stub Butterworth Pulse Shaping Filter Components

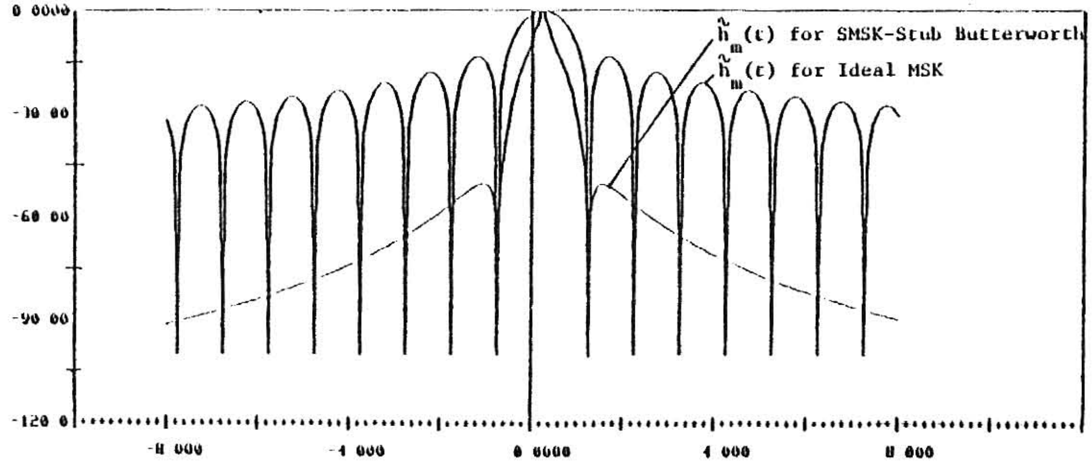

Figure 20b. SMSK-Stub Butterworth Pulse Shaping Filter

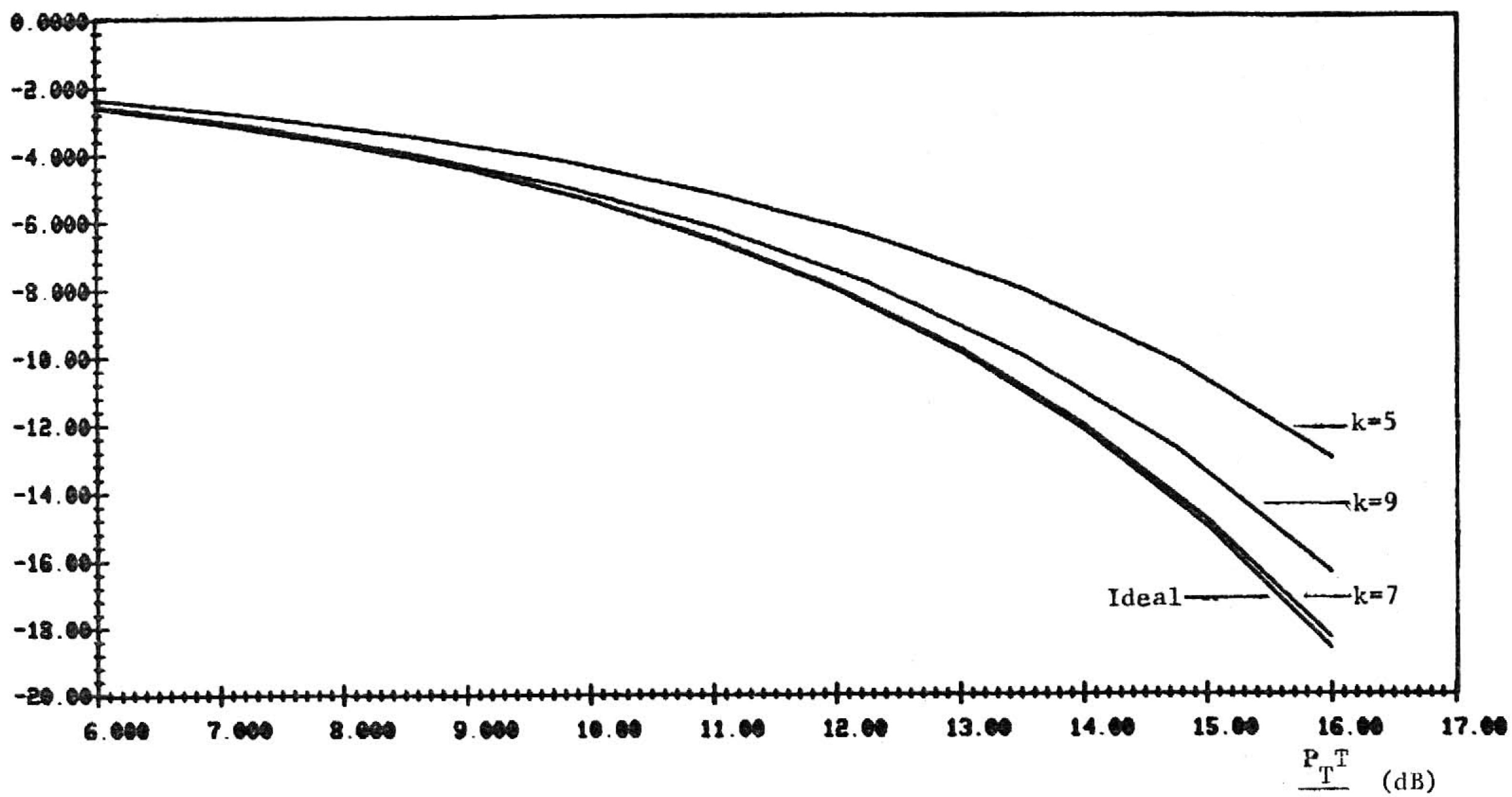

Figure 21. SMSK-Stub Butterworth Error Probability

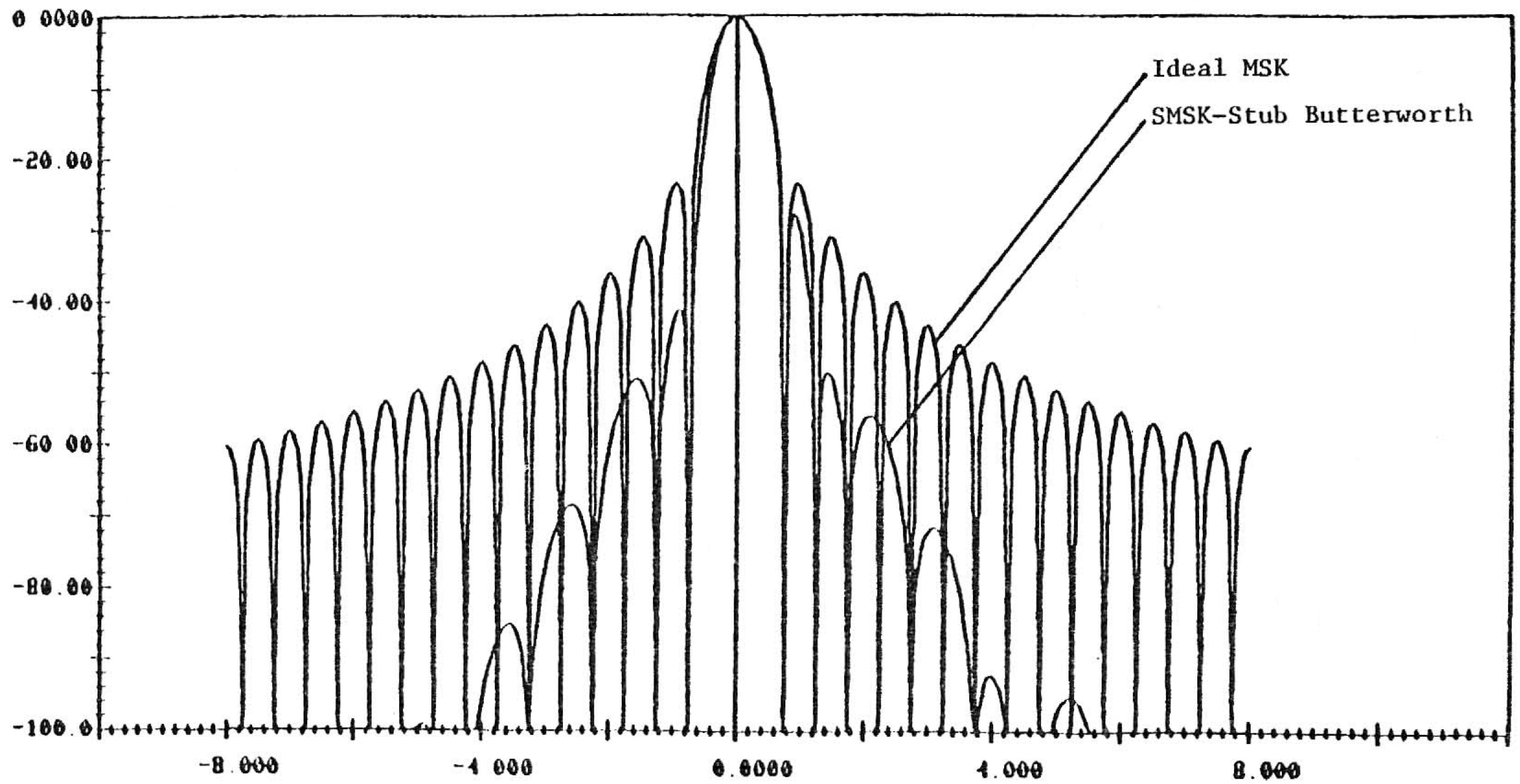

Figure 22. SMSK-Stub Butterworth Normalized Power Spectra

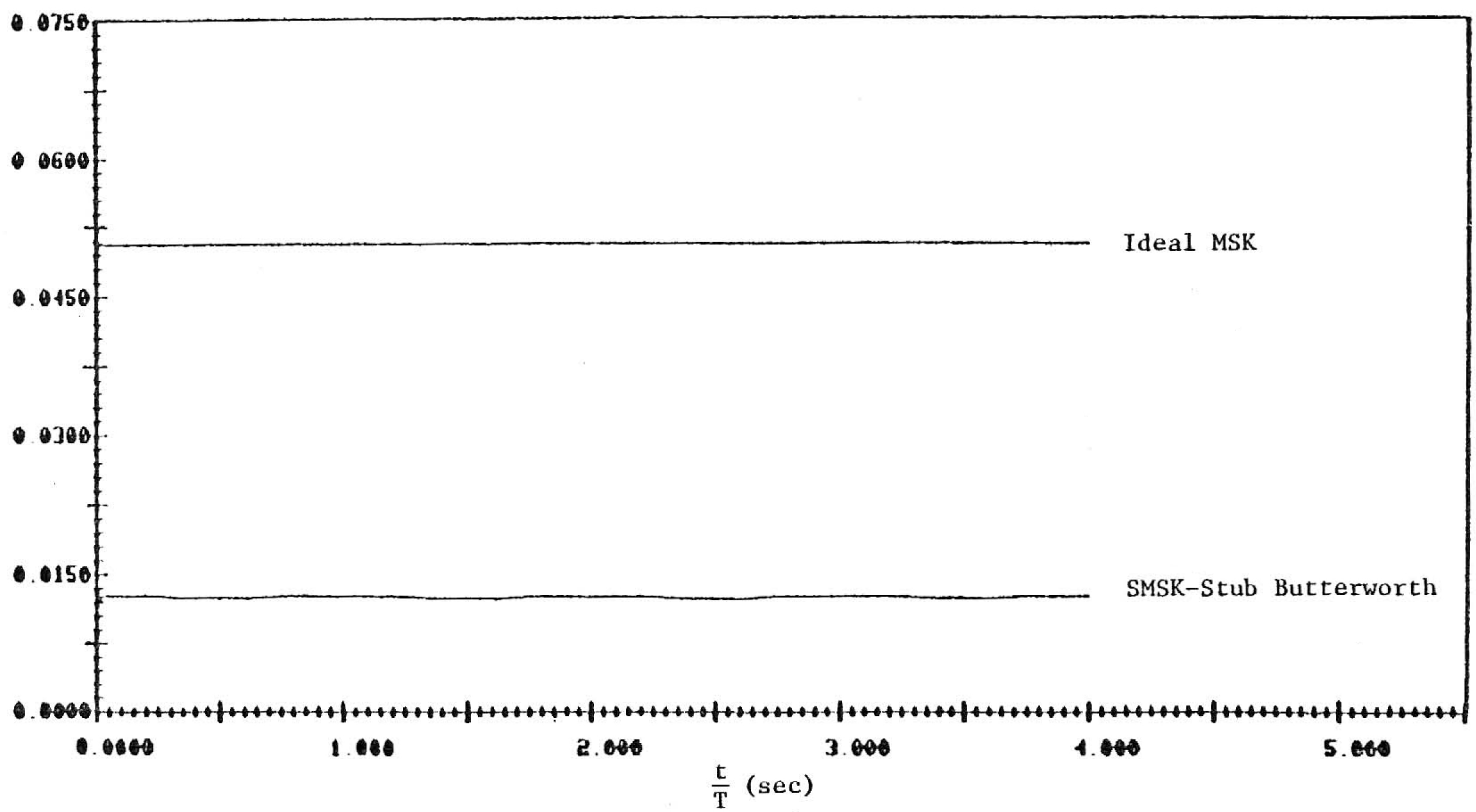

Figure 23. SMSK-Stub Butterworth Signal Envelope

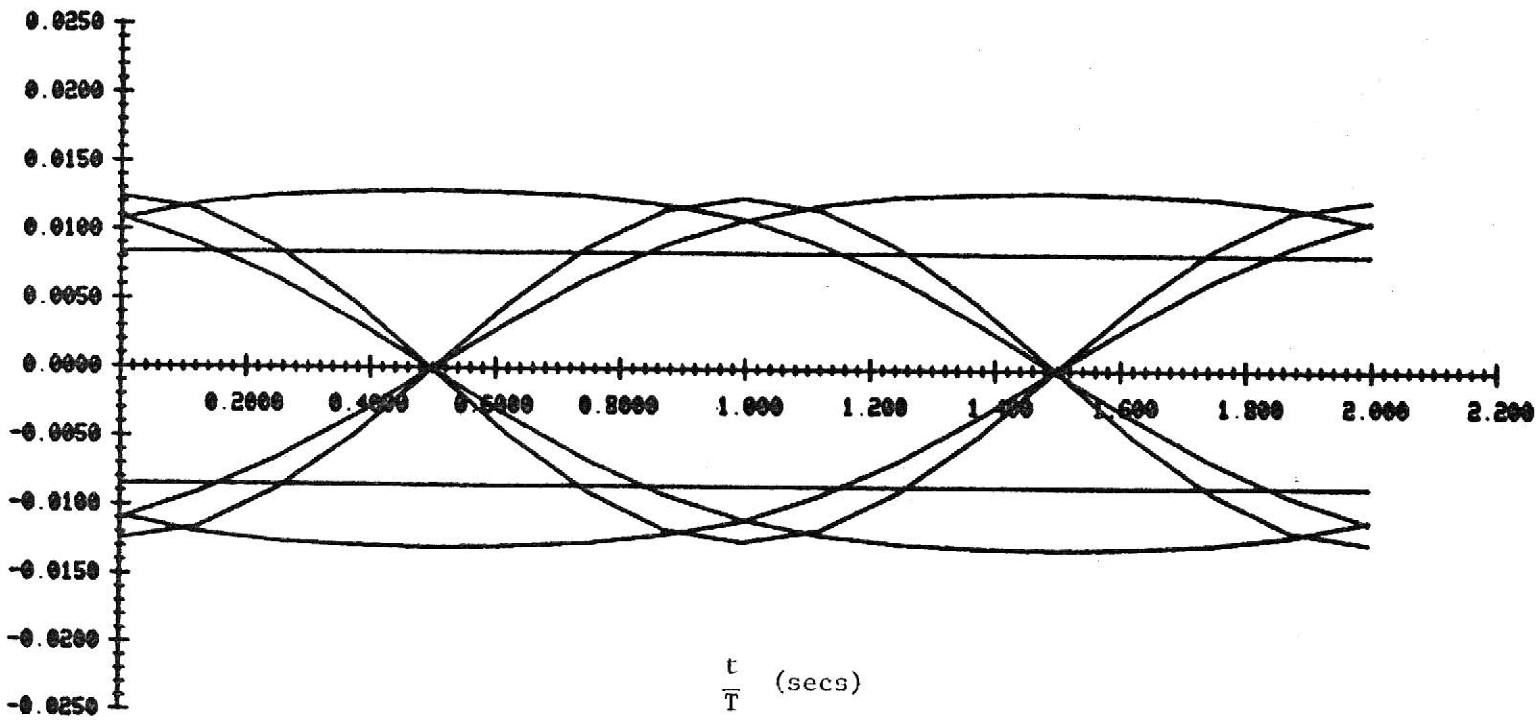

Figure 24. SMSK-Stub Butterworth Eyepattern, k=5, R=0.65

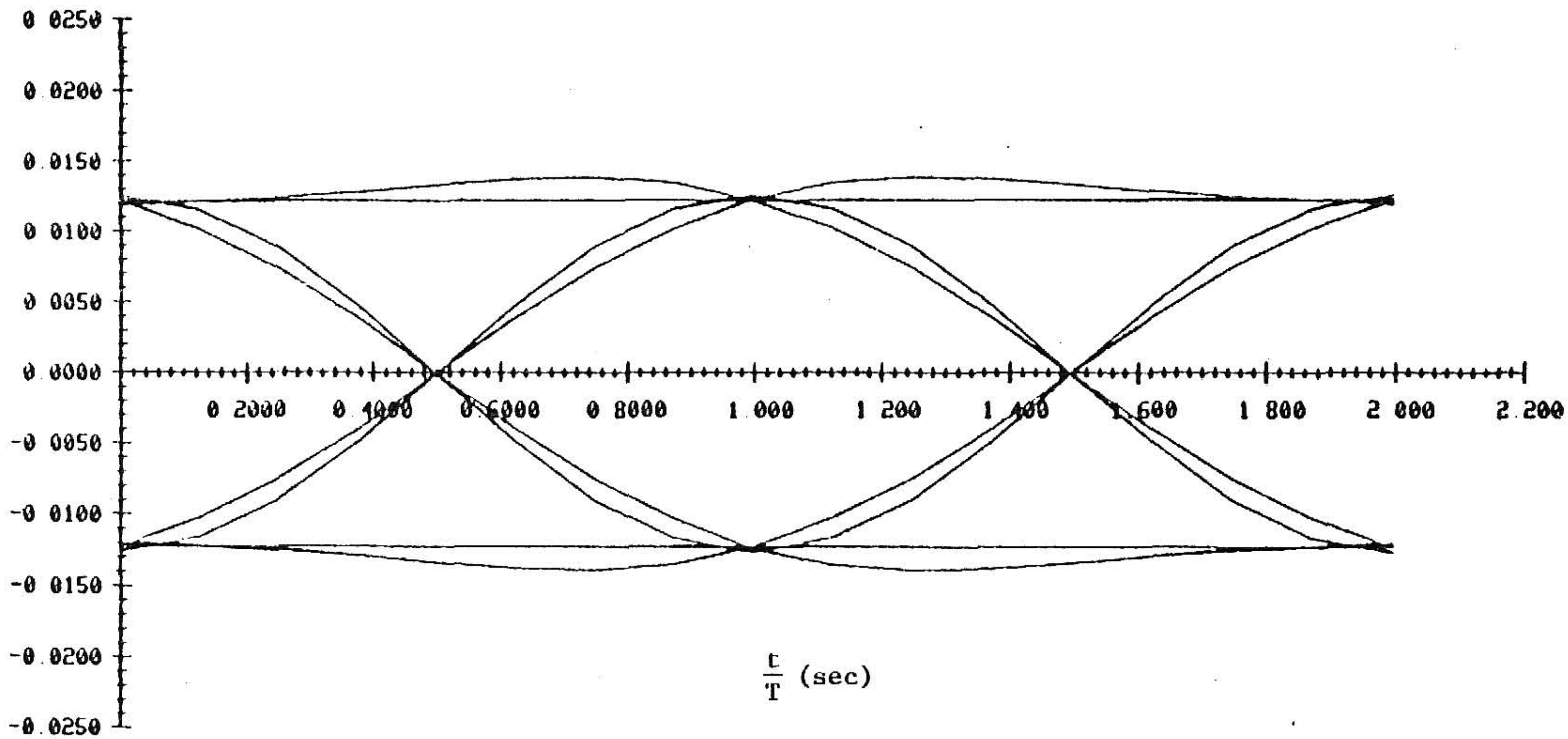

Figure 25. SMSK-Stub Butterworth Eye Pattern, k=7, R=0.65

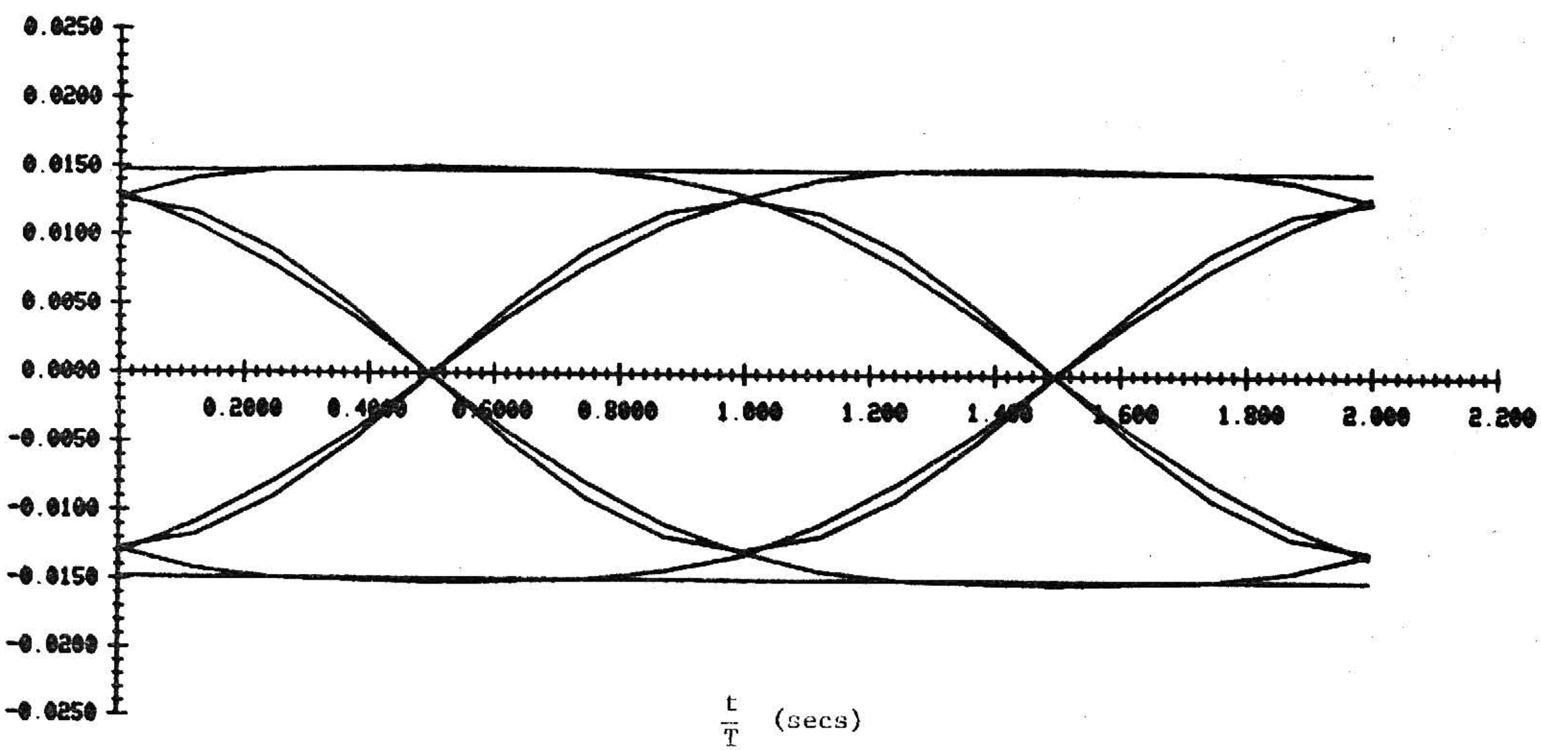

Figure 26. SMSK-Stub Butterworth Eyepattern, k=9, R=0.65

Finally, the transmitted signal is shown in Figure 27. The sub-optimum signal is slightly off-set from the ideal signal but the signal is continuous at the bit transitions.

SUMMARY

The SMSK-Stub Butterworth system demonstrated a higher degree of quality than the SMSK-Butterworth system previously discussed. Figures 28 through 30 compare the bit error probability, envelope, and power spectrum respectively. The double-notch filter, when cascaded with the Butterworth showed improvement over the Butterworth alone with respect to probability of error and constant envelope. The Butterworth system has a more compact spectrum than the stub-Butterworth system due to the fact that the Stub-Butterworth system yielded the lowest probability of error and most constant envelope when the bandwidth of the filter was slightly increase. The results show that the Stub-Butterworth is a better choice since there is little increase in complexity and out-of-band power.

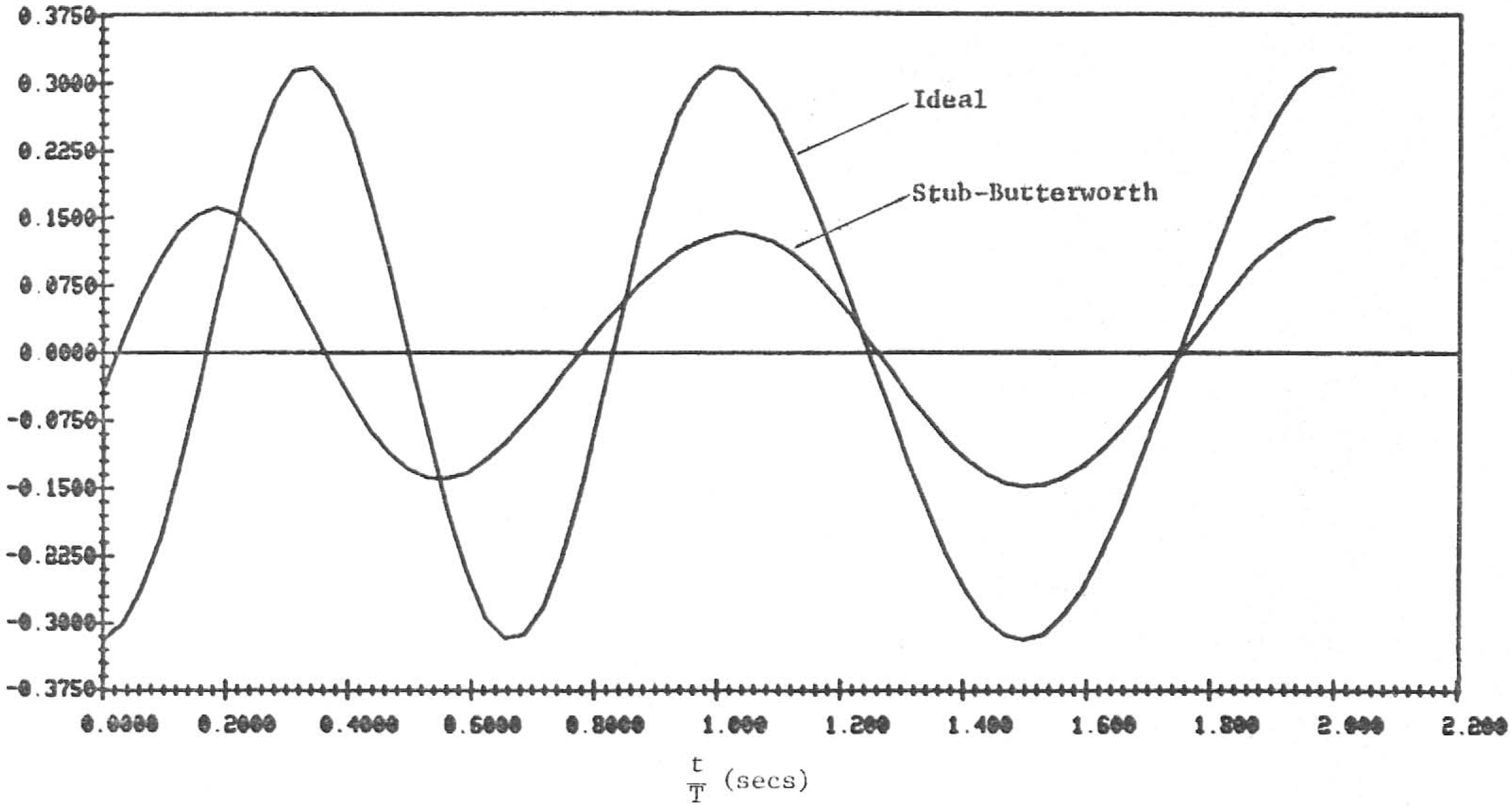

Figure 27. SMSK-Stub Butterworth Transmitted Signal

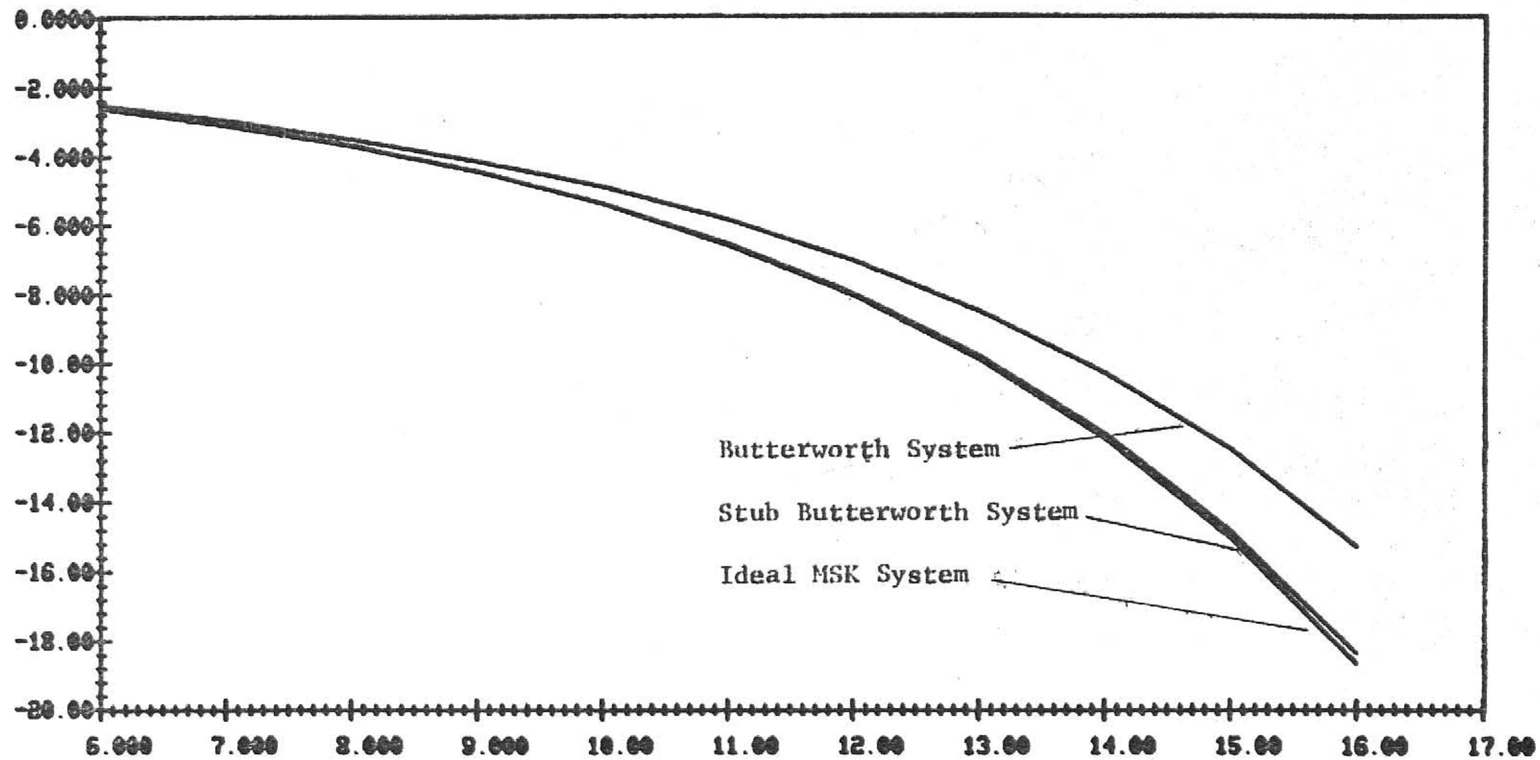

Figure 28. Error Probability Comparison

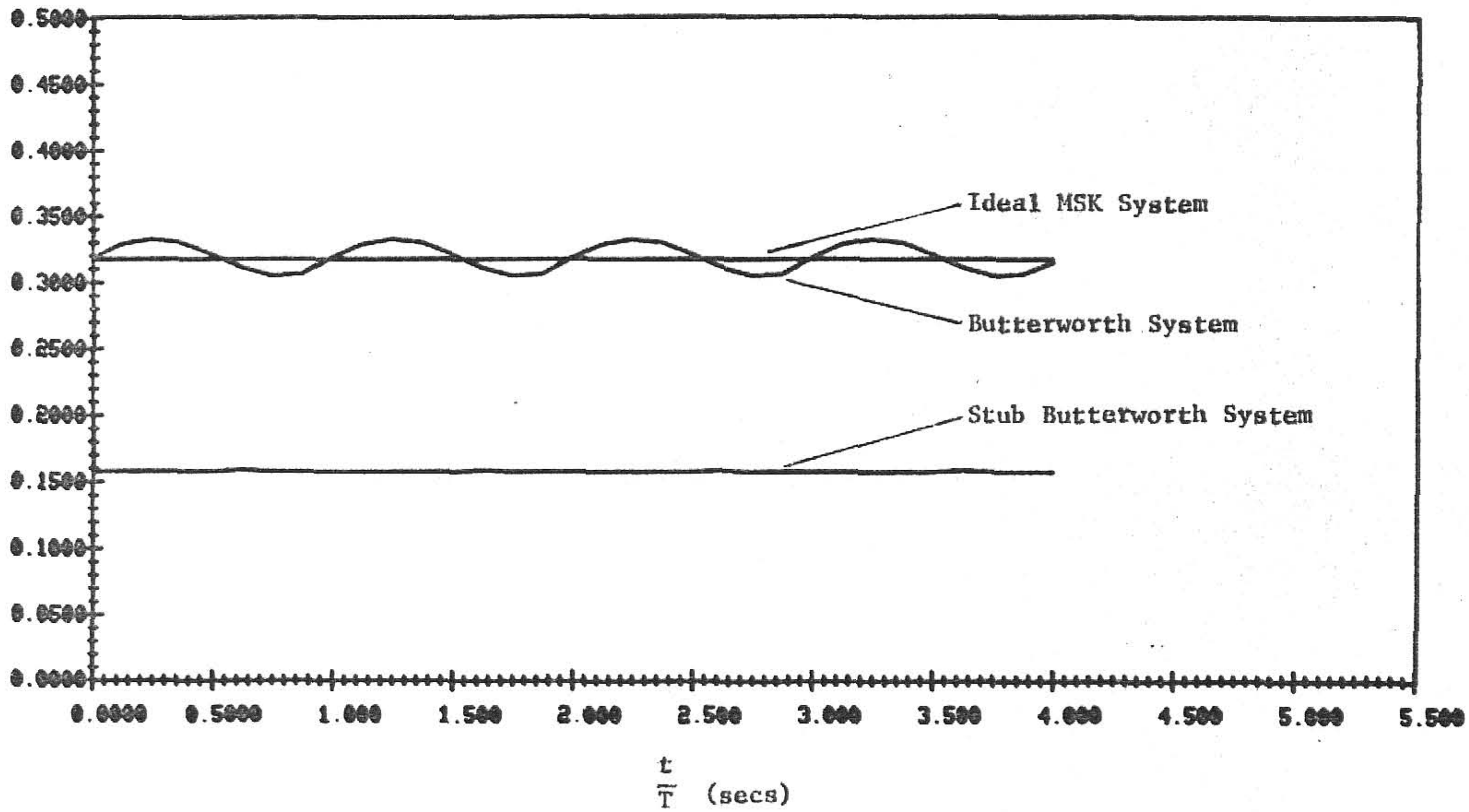

Figure 29. Signal Envelope Comparison

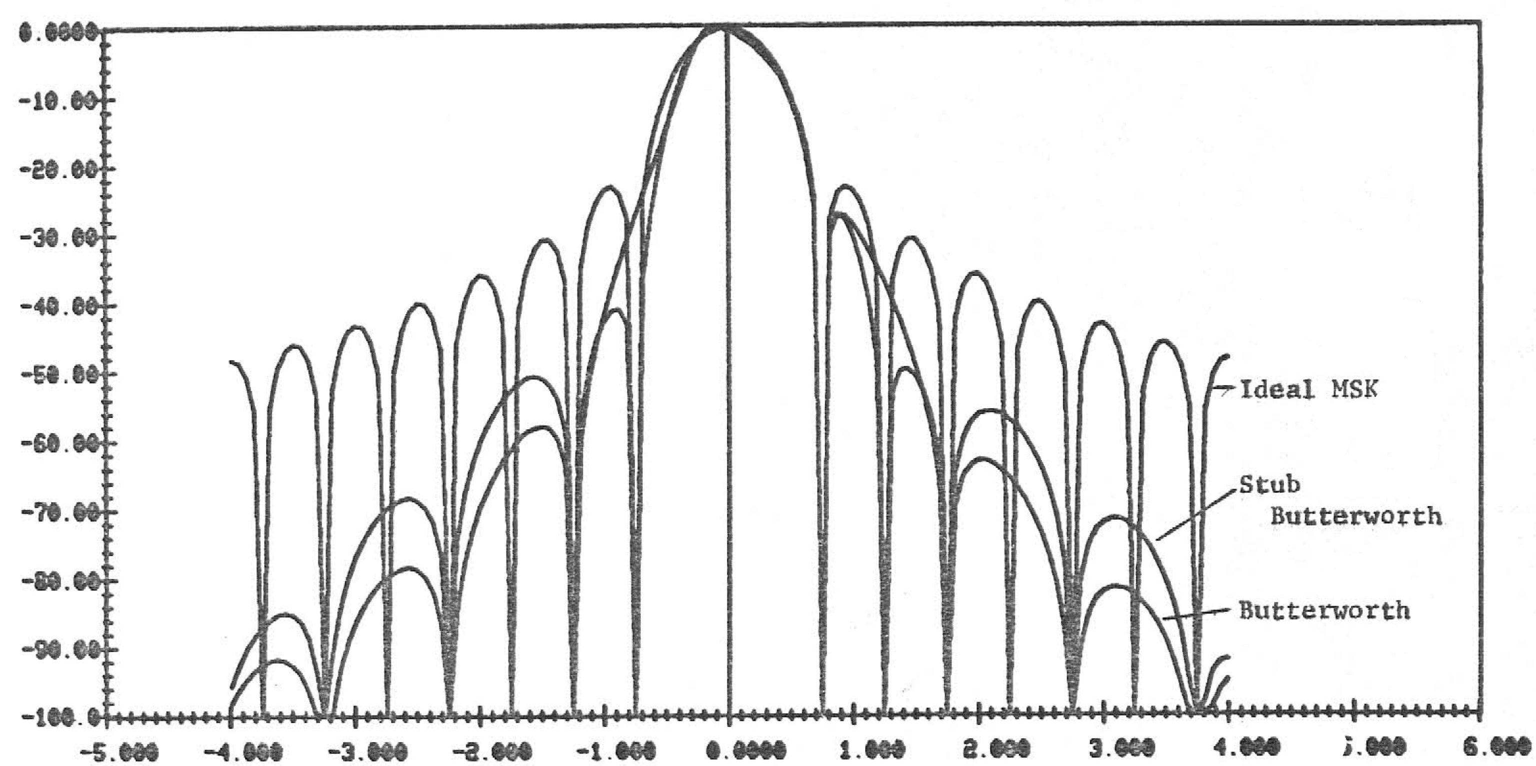

Figure 30. Power Spectra Comparison

VI. CONCLUSION

The impulse responses of the four-pole Butterworth and Stub-Butterworth filters can be synthesized much easier than the impulse response of the ideal SMSK filter. These filters offer the designer an alternative to the ideal SMSK filter with little sacrifice in performance. The results show that the Stub-Butterworth system, a configuration that is easy to construct, has essentially all the same properties as the ideal SMSK communication system.

REFERENCES

1) M. L. Doelz and E. H. Heald, Collins Radio Co., "Minimum Shift Data Communication System." U.S. Patten 2 977 417, March 28, 1961.

2) S. Pasupathy, "Minimum Shift Keying: A Spectrally Efficient Modulation," IEEE Communications Magazine, pp. 14-22, July, 1979.

3) F. Amoroso and J. A. Kivett, "Simplified MSK Signaling Technique," IEEE Transactions on Communications, Vol. COM-25, No. 4, pp. 433-441, April, 1977.

4) D. R. Hummels and F. W. Ratcliffe, "Modeling Digital Communication Systems For Numerical Evaluation of Error Rate, Power Spectrum, Eye Pattern, and Envelope." Final Report to Motorola, Inc., Kansas State University, Engineering Experiment Station, Project 2732, Nonlinear Channel Models, July, 1980.

5) M. Schwartz, W. R. Bennett, and S. Stein, Communication Systems and Techniques, McGraw-Hill, Inc., New York, 1966.

6) E. Y. Ho and Y. S. Yeh, "A New Approach for Evaluating the Error Probability in the Presence of Intersymbol Interference and Additive Gaussian Noise," The Bell System Technical Journal, Vol. 49, No. 9, pp. 2249-2265, November, 1970.

7) S. Benedetto, E. Biglier, and R. Daffara, "Performance of Multilevel Baseband Digital Systems in a Nonlinear Environment," IEEE Transactions on Communications, Vol. COM-24, pp. 1166-1175, October, 1976.

8) Reference Data for Radio Engineers, Sixth Ed., Howard W. Sams and Co., Inc., 1979.

9) R. Debuda, "Coherent Demodulation of Frequency-Shift Keying with Low Deviation Ratio," IEEE Transactions on Communications, pp. 429-435, June, 1972.

ACKNOWLEDGEMENTS

Many people assisted in some way in the development of this thesis project and thanks are in order. Standout contributors are, Fred Ratcliffe and Connie Adams, who gave the insight greatly needed to operate the Nova, and my wife, whose tolerance was desperately needed. Much guidance was needed during the course of this project and special thanks is given to Dr. Hummels.

EVALUATION OF FILTERS FOR SERIAL
GENERATION OF MSK SIGNAL

by

Patrick R. Tatum

B.S., Kansas State University, 1979

AN ABSTRACT OF A MASTER'S THESIS

submitted in partial fulfillment of the

requirements for the degree

MASTER OF SCIENCE

Department of Electrical Engineering

KANSAS STATE UNIVERSITY
Manhattan, Kansas
1981

ABSTRACT

The performance of a sub-optimum MSK system is evaluated and compared to that of an ideal system. The modulator studied uses a serial approach to MSK signal generation. The configuration studied is sub-optimum in that the transmitter filters considered are relatively simple approximations to that required for an ideal MSK system. Two filter forms were considered, a four-pole Butterworth filter and a cascaded filter consisting of a four-pole Butterworth filter followed by a double-notch filter. Both filters showed a performance comparable to ideal MSK with the cascaded filter coming very close. The performance comparisons given include calculation of error rate, envelope, eye pattern, power spectrum, and signal waveform.